

**ECONOMIC GEOLOGY
RESEARCH INSTITUTE
HUGH ALLSOPP LABORATORY**

**University of the Witwatersrand
Johannesburg**

**CHROMITITES OF THE BUSHVELD COMPLEX-
PROCESS OF FORMATION AND PGE ENRICHMENT**

**J.A. KINNAIRD, F.J. KRUGER, P.A.M. NEX and
R.G. CAWTHORN**

UNIVERSITY OF THE WITWATERSRAND
JOHANNESBURG

**CHROMITITES OF THE BUSHVELD COMPLEX –
PROCESSES OF FORMATION AND PGE ENRICHMENT**

by

J. A. KINNAIRD, F. J. KRUGER, P.A. M. NEX AND R.G. CAWTHORN

*(Department of Geology, School of Geosciences, University of the Witwatersrand,
Private Bag 3, P.O. WITS 2050, Johannesburg, South Africa)*

**ECONOMIC GEOLOGY RESEARCH INSTITUTE
INFORMATION CIRCULAR No. 369**

December, 2002

CHROMITITES OF THE BUSHVELD COMPLEX – PROCESSES OF FORMATION AND PGE ENRICHMENT

ABSTRACT

The mafic layered suite of the 2.05 Ga old Bushveld Complex hosts a number of substantial PGE-bearing chromitite layers, including the UG2, within the Critical Zone, together with thin chromitite stringers of the platinum-bearing Merensky Reef. Until 1982, only the Merensky Reef was mined for platinum although it has long been known that chromitites also host platinum group minerals. Three groups of chromitites occur: a Lower Group of up to seven major layers hosted in feldspathic pyroxenite; a Middle Group with four layers hosted by feldspathic pyroxenite or norite; and an Upper Group usually of two chromitite packages, hosted in pyroxenite, norite or anorthosite. There is a systematic chemical variation from bottom to top chromitite layers, in terms of Cr : Fe ratios and the abundance and proportion of PGE's. Although all the chromitites are enriched in PGE's relative to the host rocks, the Upper Group 2 layer (UG2) shows the highest concentration. Detailed studies of $^{87}\text{Sr}/^{86}\text{Sr}$ isotope variations undertaken on interstitial plagioclase from chromitites and different silicate host rocks show that the magma from which the chromitites formed (interstitial plagioclase $\text{Sr}_i < 0.7099$) usually differed radically from the resident liquid from which the immediate footwall rocks crystallised (Sr_i c. 0.7060 - 0.7064). These high Sr-isotope ratios can only have been produced by sudden and extensive contamination by an extremely radiogenic component. The only viable source for this component in the chamber is the felsitic roof rocks or a granophyric roof-rock melt. It is suggested that such contamination occurred when a new magma influx penetrated the residual liquid and interacted with the overlying roof-rock as well as mixing with the resident liquid. The model envisages that chromite cascaded to the floor, together with a small amount of magma adherent to the chromite or entrained within the slurry to produce interstitial silicates with enriched isotopic ratios. The close correspondence of chromitite and PGE enrichment strongly suggests that the contamination process that resulted in chromite formation also triggered precipitation of the PGE's. The base of each major chromitite layer marks the point where there was a substantial injection of new magma into the chamber, which resulted in erosion of the cumulate pile, interaction with roof rocks and inflation of the chamber. Thus, the major PGM and chromitite ore deposits of the Bushveld Complex are unconformity related, and are associated with mixing of new magma, coupled to simultaneous contamination by granophyric roof-rock melt. The chromitites, therefore, represent the products of a roof contamination and magma mixing process.

_____oOo_____

**CHROMITITES OF THE BUSHVELD COMPLEX –
PROCESSES OF FORMATION AND PGE ENRICHMENT**

CONTENTS

	Page
INTRODUCTION	1
GENERAL GEOLOGY	1
OCCURRENCE OF CHROMITITES	3
MAGMATIC EVOLUTION	7
STRONTIUM ISOTOPE STUDIES ON PLAGIOCLASE FROM SILICATE ROCKS AND CHROMITITE LAYERS	8
ISOTOPIC RESULTS	11
MODELS FOR THE FORMATION OF CHROMITITES	14
Previous models	14
PROPOSED MODEL FOR CHROMITITE FORMATION BASED ON STRONTIUM ISOTOPE DATA	16
DISCUSSION	18
ROLE OF MAGMA MIXING AND CHROMITITE FORMATION IN THE CONCENTRATION OF PGE'S	19
CONCLUSIONS	21
ACKNOWLEDGEMENTS	22
REFERENCES	22

_____oOo_____

Published by the Economic Geology Research Institute
(incorporating the Hugh Allsopp Laboratory)
School of Geosciences
University of the Witwatersrand
1 Jan Smuts Avenue
Johannesburg
South Africa

<http://www.wits.ac.za/egru/research.htm>

ISBN 1-86838-324-5

CHROMITITES OF THE BUSHVELD COMPLEX – PROCESSES OF FORMATION AND PGE ENRICHMENT

INTRODUCTION

Because of the metallurgical difficulties in extracting platinum group elements (PGE's) from chromitite horizons, until 1982 only the Merensky Reef was mined for platinum, although it has long been known that chromitites also host PGE's.²⁸ Although all the chromitites are enriched in PGE's relative to the host rocks, the Upper Group 2 layer (UG2) shows the highest concentration. PGE enrichment in chromitite layers led to the suggestion of causal relationship between the two, although a direct link has been questioned because of the lack of good PGE grade in UG1 and UG3 chromitites, the high PGE grade of the Merensky Reef, which only has thin associated chromitites,¹⁶ and the paucity of chromite in the Platereef.⁸³ In addition Maier and Barnes,⁴⁸ analysed a large number of samples and argued that there was no correlation between PGE content and chromite abundance. The purpose of this circular is to show that it is the *process* of chromitite formation that is so important in understanding how PGE's may be concentrated, not the absolute amount of chromitite that formed.

GENERAL GEOLOGY

The 2.05 Ga old Bushveld Complex covers an area of *c.* 65,000 km² and is intruded into the Transvaal Supergroup of sedimentary and volcanic rocks (Fig. 1). The Complex comprises a suite of layered ultramafic/mafic rocks, up to 9 km thick, (known as the Rustenburg Layered Suite), roofed by Rooiberg Group felsitic volcanics and granophyres and a suite of late

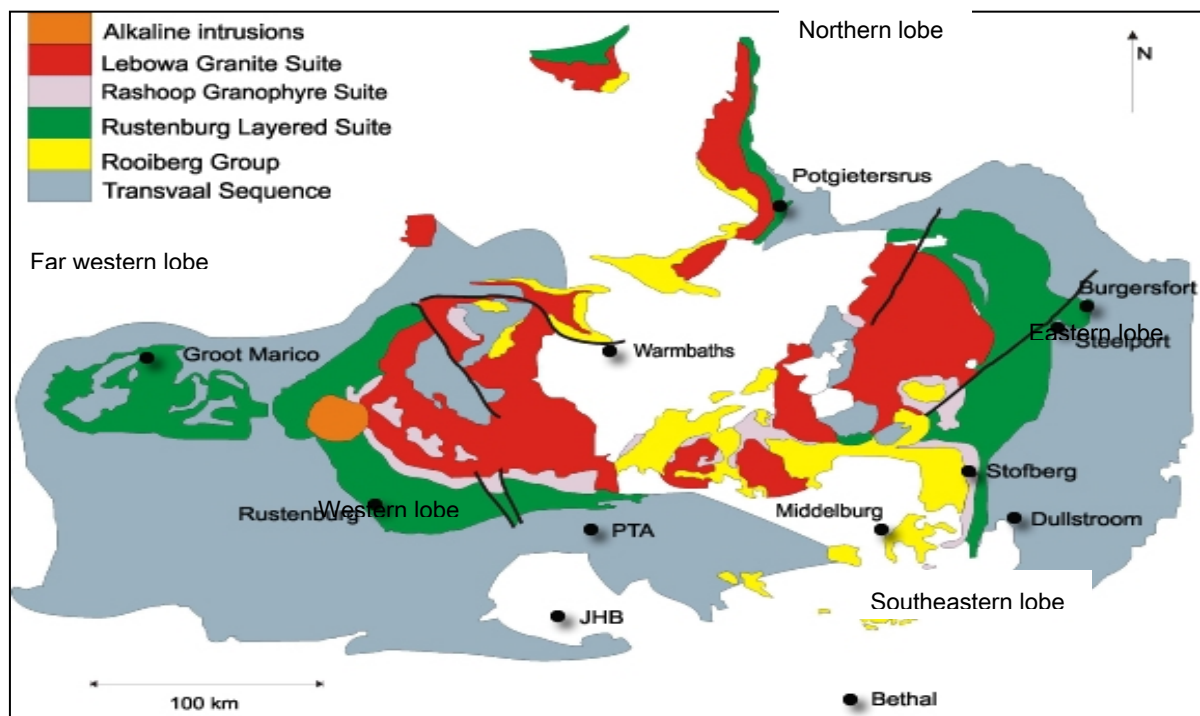


Figure 1: Generalised geological map of the Bushveld Complex.

Bushveld granites. The layered suite is preserved in five lobes, the far-western, western, eastern and northern lobes, which may have been connected to each other and linked to a feeder chamber at depth (Fig. 1). Little is known about the fifth southeastern lobe that is

obscured by younger sediments. The stratigraphy in the eastern and western lobes is broadly similar although there are significant differences in terms of thickness and detailed lithological variations.

The Rustenburg Layered Suite (RLS), which ranges in composition from dunite to ferrodiorite, is subdivided into Marginal (MaZ), Lower (LZ), Critical (CZ), Main (MZ) and Upper (UZ) Zones (Fig. 2). The exact boundaries of the zones differ, however, according to whether they are drawn on the basis of mineralogical changes due to differentiation or on an isotopic basis.³⁷

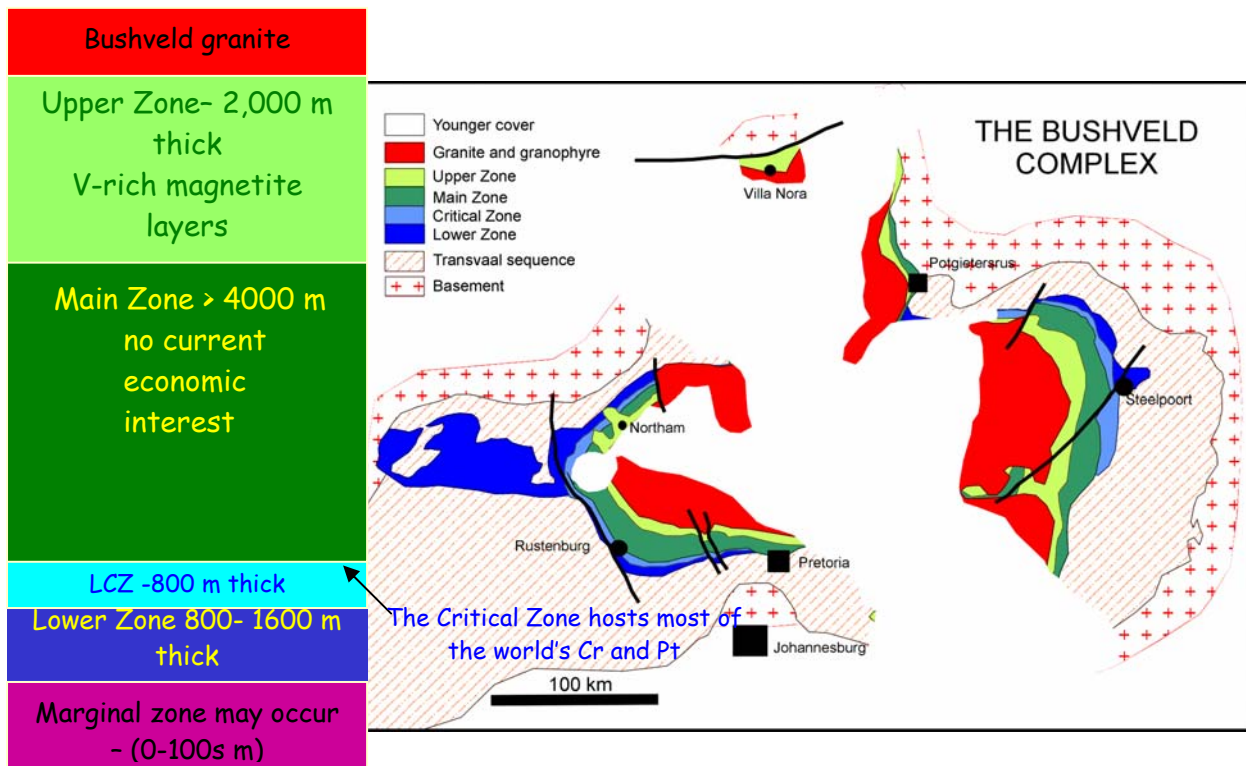


Figure 2: Subdivisions of the Rustenburg Layered Suite, showing the zones of economic interest.

The MaZ, which is not always present, together with related sills, comprises up to 880 m of heterogeneous noritic rocks along the basal contact of the Complex. The LZ comprises dunites, harzburgites and pyroxenites, with the thickest sections developed in the central sector of the eastern lobe, near the Union Section in the western lobe, in the far-western lobe and south of Potgietersrus in the northern lobe.

The CZ, which is characterised by spectacular layering, hosts world-class chromite and platinum deposits in several different layers (termed reefs). The Critical Zone, is divided into a lower subzone (C_LZ), which is entirely ultramafic and is characterised by a thick succession of orthopyroxenitic cumulates and an upper subzone (C_UZ) that comprises packages of chromitite, harzburgite, pyroxenite, through norite to anorthosite. Subdivision into magmatic cycles is somewhat subjective, but nine cycles have been recognised in the C_LZ and eight cycles in the C_UZ .⁶⁶ The transition from C_LZ to C_UZ occurs at the base of the lowermost anorthositic layer of the RLS between two chromitite layers.

Two distinctive cyclic units, the Merensky and Bastard units are included within the CZ of the original classification⁶¹. However, a significant break in the initial Sr isotope ratio, and a major unconformity at the base of the Merensky Unit,⁴⁰ led Kruger³⁷ to draw the boundary between the CZ and MZ at the base of the Merensky Unit, where the major magma influx occurs, rather than at the top of the Giant Mottled Anorthosite, a distinctive layer characterised by large oikocrysts of pyroxene at the top of the Bastard Unit.

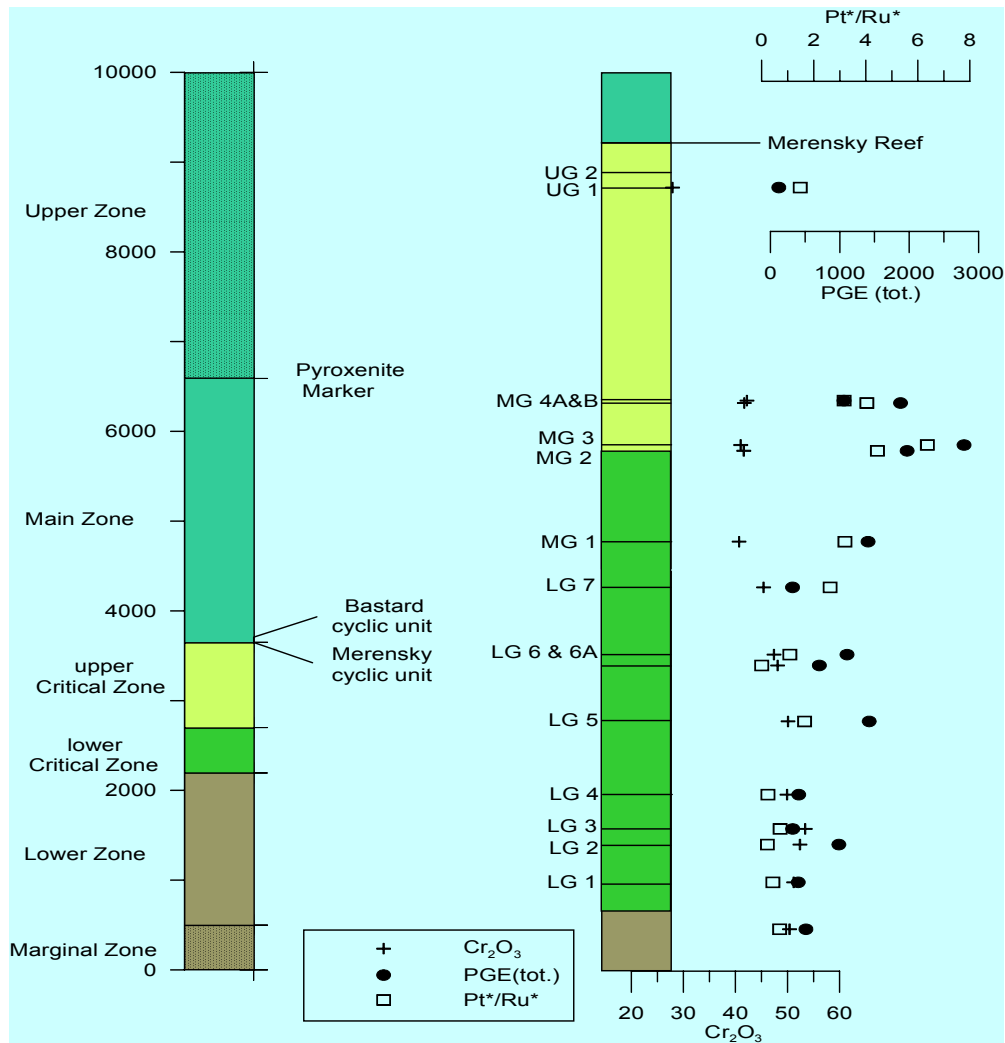
The MZ, which is the thickest zone of the Layered Suite (*c.* 3500 m), comprises a succession of gabbro-norites in which olivine and chromite are absent and anorthosites are rare. Although not as spectacularly layered as the CZ, discrete packages of modally layered rocks can be identified.^{52,51, 57}

The UZ is some 2000 m thick and is characterised by up to 25 magnetite layers in four groups and lithologies of anorthosite, troctolite and ferrogabbro to diorite. The mineralogical base of the UZ is defined as the first appearance of cumulus magnetite,⁶¹ although Kruger³⁷ has redefined the base at the Pyroxenite Marker, a prominent orthopyroxene-bearing horizon a hundred or more metres below the first appearance of cumulus magnetite, on the basis of an abrupt break in Sr-isotope ratios at another major unconformity.⁶⁹

The Rustenburg Layered Suite has a sill-like character although floor rocks control the geometry. The Lower Zone is discontinuous and the Critical and Main Zones transgress the floor rocks in places in the eastern Bushveld (Fig. 2). Transgressive relationships are also present between Main and Upper Zones.^{37,84} Scoon and Teigler⁶⁷ divided the eastern Bushveld Complex into different sectors that are structurally distinct; the central sector comprises a complete succession from LZ, through the CZ to the overlying MZ and UZ. South of the Steelpoort Lineament, in the southern sector, the succession is considerably different. The LZ is entirely absent, the CZ and MZ occur, but the CUZ, although complete, is much thinner than to the north.⁶⁷ Similarly, the western lobe can be divided into six different compartments each of which is structurally controlled and has an unique lithostratigraphy.⁶⁶

OCCURRENCE OF CHROMITITES

Chromitites are almost entirely restricted to the CZ, although in the northern lobe, south of Potgietersrus, there are minor occurrences in the LZ. The chromitite layers occur in three stratigraphically delineated groups,²² each composed of several layers and numbered from the base upwards (Fig 3.). The Lower Group (LG) consists of up to seven layers hosted in feldspathic pyroxenite, the thickest being the LG6 layer, also known as the Steelpoort seam.⁶⁵ The LG1 to LG4 chromitites are often associated with olivine, a feature that distinguishes them from overlying chromitites, which are invariably olivine-free.³² Four chromitites comprise the Middle Group although multiple layers of each may develop, for example the MG1 may consist of two thinner chromitites below a 1m thick chromitite and at Tweefontein Mine in the eastern Bushveld a chromitite designated MG0 is locally developed below the MG1. The MG group straddles the boundary between the lower Critical Zone and the Upper Critical Zone and by convention, MG1 and MG2 lie below the first anorthosite, and MG3 and MG4 are above. The Upper Group usually consists of two chromitites (UG1 and UG2 – see Fig. 4), although in the eastern Bushveld, UG3 and UG3a layers are also recognised. The UG1 is world renowned for the bifurcations of individual chromitite layers although locally the UG2 and LG5 may also show significant development of bifurcations. In



any given locality, there may be a significant variation in number of chromitite layers within a vertical package, and in the AM38 core discussed here 30 individual chromitite layers can

Figure 3: Stratigraphy showing the generalised thickness of the zones within the Rustenburg Layered Suite, Bushveld Complex. The column on the right shows the position of the major chromitite layers within the Critical Zone. The percentage of Cr_2O_3 in chromite is shown together with PGE compositional data for each of the chromitite layers based on Scoon and Teigler (1994). $\text{Pt}^* = \text{Pt} + \text{Pd} + \text{Rh}$; $\text{Ru}^* = \text{Ru} + \text{Ir} + \text{Os}$.

be distinguished between LG5 and MG4.

Two-to-four thin chromitite layers (each 1-20 mm) define the upper and lower limits of the main economic mineralisation of the Merensky Reef, with the greatest concentrations near the upper chromitite.⁴³ Although the Platereef, which occurs in the northern lobe of the Bushveld Complex, is widely regarded as an equivalent to the Merensky Reef, the chromite distribution is sporadic in comparison to the thin, but persistent chromitite stringers associated with the Merensky Reef. There is a considerable lateral variation in the occurrence and thickness of the chromitite layers in the different lobes and also between the northern and southern portions of the eastern and western lobes. Cawthorn and Webb²⁰ imply continuity of individual layers over more than 300 km. Although single layers can be traced for more than km in both eastern and western lobes, it may be the package of chromitite that is laterally continuous over long distances, rather than an individual layer. Correlation of chromitites is

based largely on interlayer silicates and partly on the thickness of the chromitite but in some areas chromitite horizons are missing or correlation may be tenuous.³² In the western and eastern lobes for example the LG group is well developed in the northern sector and poorly



Figure 4: Upper Group chromitite layers. On the left bifurcating UG1 chromitite layers separated by mottled anorthosite with dendritic clinopyroxene, Dwars River eastern Bushveld. On the right, plagioclase-rich UG2 chromitite, Rustenburg area.

developed in the southern sector of each lobe and Scoon and Teigler⁶⁷ documented considerable lithostratigraphic variation in the LG6 over only 2 km of strike. In the eastern Bushveld, north of the Steelpoort Lineament in the central sector, there is a well-developed sequence of Lower Group chromitites with seven main layers (LG1-LG7), but the Middle Group chromitites (MG1- MG4) are thin and discontinuous. Upper Group chromitites (UG1 - UG3/3A), whilst persistent, are relatively thin. To the south of the Steelpoort Lineament, Lower Group chromitites are thin to absent, whereas the MG and UG packages are much thicker, although the UG 3/3A is absent.⁶⁷

Throughout the Bushveld Complex, the chromium content of the chromitite layers decreases upwards (Fig. 3). The LG6 layer has a Cr_2O_3 content of 46 – 47%, MG chromitites have 44 – 46% Cr_2O_3 and the UG2 layer has around 43% Cr_2O_3 .⁶⁵ This is reflected in the upward decrease in the Cr:Fe ratio; the LG6 layer has a Cr:Fe ratio of between 1.56 and 1.60, MG chromitites are between 1.35 and 1.50 whilst the UG2 layer has a Cr:Fe ratio of between 1.26 and 1.40. Chromite grains, which vary in size from <50 microns to > 2mm, exceed 50% of the mineral assemblage in a chromitite. The interstitial minerals change from mainly orthopyroxene in the lowest LG chromitites to orthopyroxene and plagioclase in the MG chromitites, to dominantly plagioclase with minor orthopyroxene in the uppermost UG chromitites. A poikilitic texture is frequently developed in the chromitites, where oikocrysts of pyroxene or plagioclase enclose chadacrysts of very fine-grained chromites. Accessory minerals include clinopyroxene, biotite/phlogopite, chlorite, talc, quartz, carbonates, sulphides and platinum group minerals.

The spatial association between chromitites and PGE enrichment, first noted by Hall and Humphrey in 1908²⁸, has also been noted by numerous other authors over the years.^{33,44,66,71,79,82} The UG2 contains the highest concentrations of PGE's in the various chromitite layers and grades may locally exceed 10 g/t. Fifty kilometres east of Rustenburg, Lonmin has exploited the UG2 chromitite for its PGE's since 1989, and PGE's from the UG2 presently account for 70% of Lonmin's production. Typical percentages of precious metals in the UG2 are 49.5% platinum, 22.5% palladium, 15% ruthenium, 8.7% rhodium 3.7% iridium and 0.6% gold.⁴⁷ Generalised values of PGE's in the UG2 around the Bushveld Complex are shown in Figure 5. The attractions for mining the UG2 are: (1) the elevated PGE values, which locally may equal or exceed those of the Merensky Reef; (2) its relative proximity to

the Merensky Reef in the western Bushveld (from 20 - 210m); (3) its density; and (4) the thickness of the unit, which on Lonmin varies from 0.7 to 1.3 m.

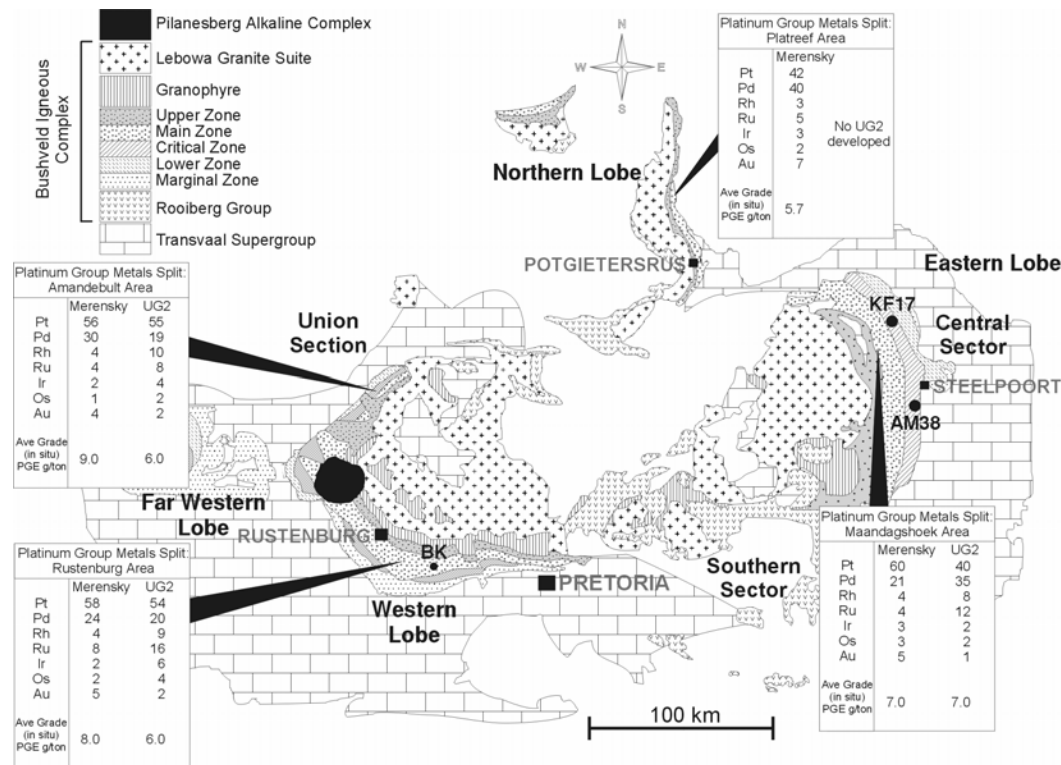


Figure 5: Geological map of the Bushveld Complex showing the different platinum group metal concentrations in the various lobes. Data on PGM concentrations combined from Buchanan (1988); Lee (1996); Barnard Jacobs Mellet (2000) plus personal communications from mines. Locations of cores AM38, KF17 and BK, discussed in this text are also shown.

In addition to the UG2 and economic PGE mineralisation associated with thin chromitite stringers at the base and top of the Merensky Reef, all other chromitites contain lower, but significant, concentrations of PGE's.^{44,66,71,79} However, there does seem to be a variation in PGE proportions in the chromitites according to the host rock. Whereas the Ru-Os-Ir group consistently occurs there is a low abundance of the Pt-Pd-Rh in the pyroxenite-hosted LG's and MG1- MG2.^{44,66} In contrast, chromitites higher in the stratigraphic succession (MG3, MG4 and UG1), which occur in plagioclase-bearing rocks, are more enriched in Pt-Pd-Rh.^{44,66,79} A relationship has also been noted between PGE content and modal chromite with the Pt-Pd-Rh declining relative to Ru-Os-Ir when chromite constitutes more than 75% volume of the rock.⁷⁷ Scoon and Teigler⁶⁶ subdivided chromitites into subgroups according to their host and chemistry. Chromitites in harzburgite-pyroxenite cycles with Cr:Fe ratios >1.8 have a low total PGE content (<1000 ppb) and (Pt+Rh+Pd)/(Ru+Ir+Os) <1. Chromitite in pyroxenite-norite-anorthosite cycles with Cr:Fe <1.5 have a higher PGE content (1000-5000 ppb) and Pt+Rh+Pd/Ru+Ir+Os >2.

All chromitites beneath the Merensky Reef are poor in base metal sulphides in spite of elevated PGE concentrations. Chromitites below MG2 have only trace sulphur, whereas MG2-UG1 have 0.01-0.02% S.⁶⁶ The chromitite layers of the Bushveld Complex host platinum group elements as platinum group minerals (PGM), which principally include the

PGE-sulphides laurite, braggite and cooperite, together with antimonides (geversite, stibiopaladinite), arsenides (sperrylite), bismuthides (insizwaite), tellurides (merenskyite, moncheite) and alloys (isoferro-platinum), with some base metal (Ni-Cu-Fe) sulfides.⁴³ In general, the greater part of the PGM present within chromites appear to be in submicroscopic grains of PGE and base metal alloys, despite the predominance of sulphide phases at the microscopic scale.^{63,2}

MAGMATIC EVOLUTION

The filling of the magma chamber occurred over a period of *c.* 75 Ka.¹⁹ Early Sr-isotopic data were instrumental in demonstrating the multiple intrusive nature of the RLS and the close association of intrusion with mineralisation, particularly at the level of the Merensky Reef.^{29,38,40} According to Kruger,³⁹ the RLS as a whole can be viewed as having three main magmatic lineages – the Lower and Critical Zone harzburgite-to-noritic lineage (with a low Sr ratio from 0.705 – 0.7064), the Main Zone gabbro-norite lineage (with high Sr ratio *c.* 0.7082) and the Upper Zone Fe-rich gabbro-norite lineage (with Sr ratio *c.* 0.7075). The boundaries between these major magmatic episodes are major unconformities within the magma chamber, coincident with the base of the Merensky Reef and the Pyroxenite Marker (Fig. 3). However, isotopic evidence also suggests that during the formation of the Lower and Critical Zones there were repeated influxes of new magma, which expanded the chamber both upwards and outwards.

Kruger,³⁹ following Wager and Brown,⁸¹ suggested that the evolution of the Bushveld magma chamber occurred in two major stages with a lower open system “Integration stage” characterised by numerous influxes of magma of contrasting isotopic composition and concomitant accumulation of cumulates (during LZ, CZ and lower MZ), and an upper closed system “Differentiation stage” in which large-scale fractionation of two major magma influxes (the upper MZ and UZ) occurred with minimal addition of new magma within each zone. On the margins of the intrusion, the expansion of the chamber is visible as onlapping relationships (Fig. 2). Nevertheless, the RLS is a single lopolithic intrusion with a very large lateral to vertical aspect ratio of > 44:1, and the eastern and western “lobes” may have been interconnected from the start.²⁰

The isotope data indicate influx of Main Zone magma at the Merensky Reef level, which may have resulted in a 60% increase in magma volume. Similarly, the influx that initiated the Upper Zone at the Pyroxenite Marker was a further 70% relative to the residuum.⁴¹ Given the sill-like nature of the RLS, new influxes of magma spread out laterally. For the MZ and UZ magmas, this resulted in an increase in lateral extension as well as upward expansion. However, during the CZ development when chromitites formed, the pulses of magma were smaller and more frequent so that the volume of fractionating magma and residual liquid in the magma chamber at any one time is likely to have been much less than during MZ and UZ times.

The role of magma mixing in producing sulphide mineralisation, especially enrichment in PGE's in the Merensky Reef, has been previously discussed in the literature.^{13,18,37,46} In addition, magma mixing has been proposed as an important potential mechanism for chromitite formation. The purpose of this paper is to undertake a detailed isotopic examination of chromitite packages to investigate the possibility of new influxes of magma at the level of each chromitite layer and to assess the degree of crustal contamination during such influxes of new magma.

STRONTIUM ISOTOPE STUDIES ON PLAGIOCLASE FROM SILICATE ROCKS AND CHROMITITE LAYERS

Schoenberg et al.⁶⁴ showed that interstitial silicates in several chromitite layers in the Critical Zone contain significantly elevated initial Sr isotope ratios, occasionally exceeding 0.71. This is consistent with an early hypothesis of Irvine³⁴ of chromitite crystallisation from the resident magma by contamination from a siliceous material. To extend this work, three cores from different parts of the Bushveld Complex were selected for study to include lithologies extending from below the LG5 chromitite to those above the UG2 layer. Geochemical analyses of whole rocks and mineral separates have been completed together with strontium isotope analyses of plagioclase separates (Table 1). Two cores were sourced from the Steelpoort area of the eastern Bushveld, the other from Brakspruit in the Rustenburg area of the western Bushveld.

Core AM38 was obtained from south of Steelpoort. It includes chromitites from layers LG5 to MG4. The location of the core on Dwars Rivier 372 KT, which is south of the Steelpoort Lineament, is shown in Figure 5. The core extends from 10m below LG5 to 40m above MG4 (Fig. 6). Surface samples collected east of the Lydenburg road extend the sampling to *c.* 80m below the LG5. The terminology of the chromitite layers, used in Figure 6, follows that of the Avmin mining company and shows the thick chromitite at *c.* 95m depth as LG6, which seems logical given the distance below the anorthosite. However, the difficulty of correlation between chromitite layers in the Bushveld is illustrated by the fact that this thick chromitite is regarded as the MG1 by some mines south of the Steelpoort Lineament and as LG6 by others.

Core KF17, from farm Klipfontein in the central sector of the eastern Bushveld extends from approximately 10m below UG1 to the hanging wall norite above UG3, a vertical distance of 120m (Fig. 7). In the Rustenburg compartment, the BK core (Fig. 8) covers the UG1 package and includes 15 cm of hanging wall pyroxenite, two chromitite layers varying from 0.30–0.50 m thick, separated by 0.55 m of chromitiferous pyroxenite, 2.38 m of interlayered chromitite and anorthosite, and 4 m of footwall anorthosite.

Core samples were selected at regular intervals through apparently homogeneous lithologies, close to lithological boundaries, from the immediate footwall and hanging wall to the chromitite layers, as well as from the base, middle and top of the chromitite layers when possible (Figs. 6-8) and plagioclase was separated from each of the chosen samples. The plagioclase that occurs below the C_LZ - C_UZ boundary is an interstitial phase (Core AM 38, Fig. 6) whereas above and within the anorthosite it is a cumulus phase except in pyroxenites and chromitites where it is again interstitial. Plagioclase selected for study therefore includes cumulus material from anorthosite, norite, gabbro-norite and chromitiferous anorthosite and intercumulus plagioclase from pyroxenite, chromitiferous pyroxenite and chromitite. In addition plagioclase from a basic pegmatoid was also separated from KF17 core (Fig. 7).

Surface and core samples were crushed to a size fraction +100 to –125 microns and plagioclase separates were obtained from a Frantz magnetic separator. Further hand picking using a binocular microscope ensured purity of the sample. After sample dissolution in HF-HNO₃, Rb and Sr fractions were obtained using resin-packed separation columns. Rb was

loaded in chloride form onto outgassed double Ta filaments and Sr loaded with phosphoric acid onto single Ta filaments. Measurements were carried out by thermal ionisation solid

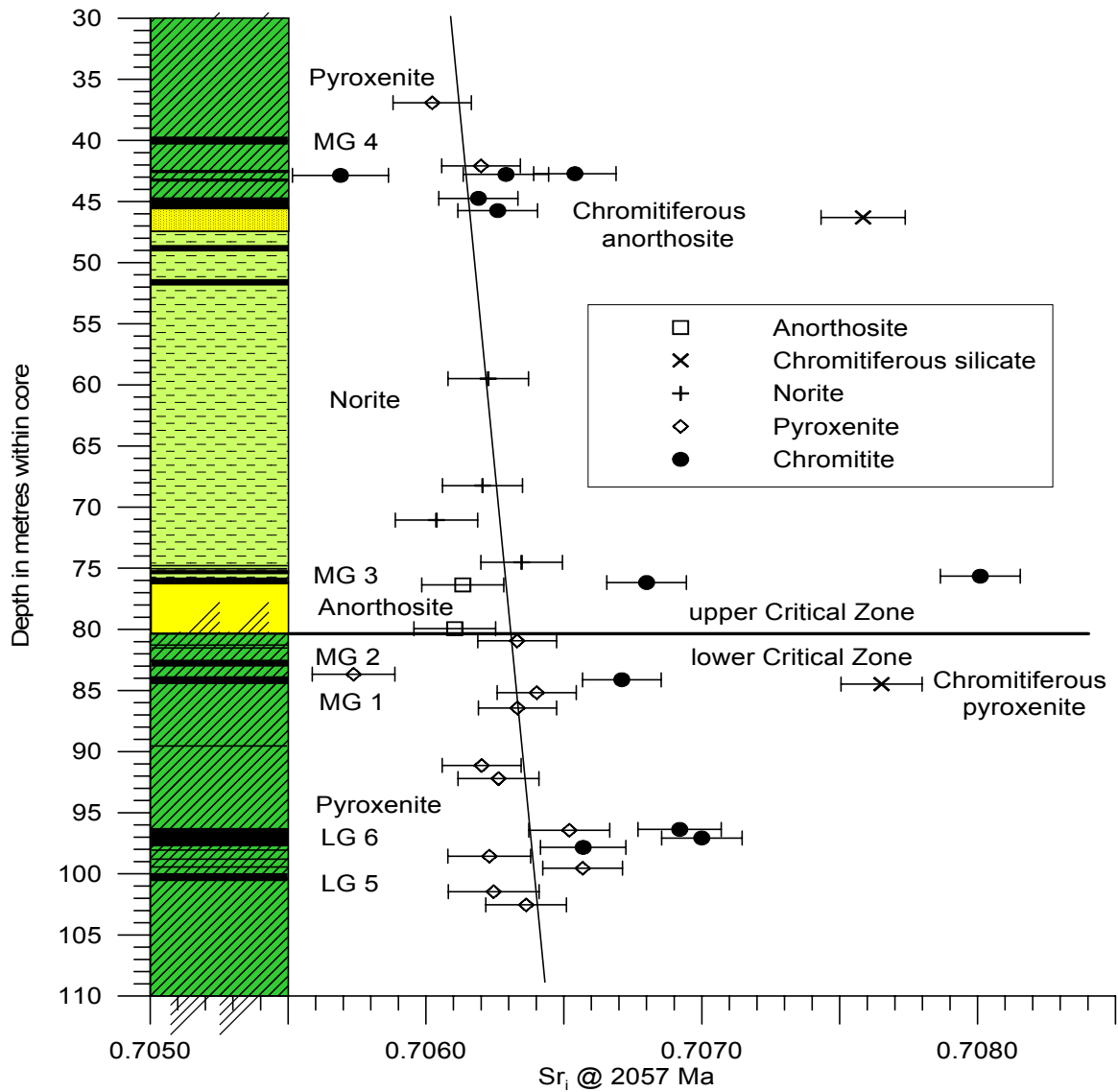


Figure 6: Initial strontium isotope ratio profile in lower-upper Critical Zone silicates and chromitites, demonstrating higher Sr_i ratios in the plagioclase from chromitites. Horizontal bars indicate 2-sigma error for Sr values. Data from AM 38 core, south of the Steelpoort lineament (see Fig. 5 for location). The MG chromitites straddle the boundary between the lower Critical Zone and the upper Critical Zone and by convention, MG1 and MG2 lie below the first anorthosite package, and MG3 and MG4 are above. The isotopic trend line illustrates the slight upward decrease in initial Sr ratio of the silicate rocks from the lower Critical Zone to the upper Critical Zone. Data for samples shown in Table 1.

source mass spectrometry at the Hugh Allsopp Laboratory of the University of the Witwatersrand.

Rb determinations were made on a VG MM30 equipped with a Keithley electrometer and Sr was analysed on a VG-354 multi-collector instrument using Pyramid TIMS software.

Corrections for fractionation and spike contribution on the $^{87}\text{Sr}/^{86}\text{Sr}$ ratio were made using an exponential law.

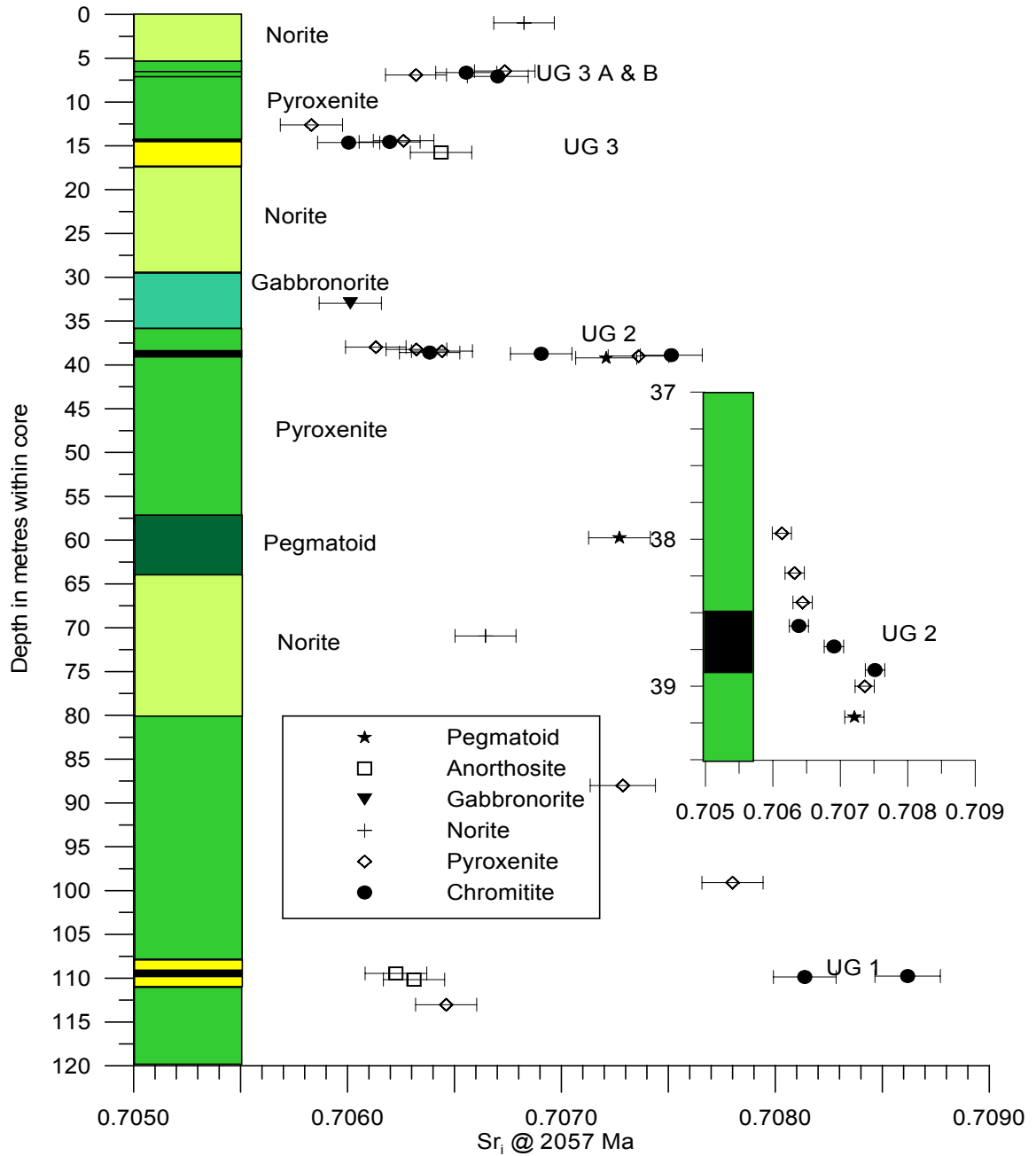


Figure 7: Initial strontium isotope ratio profile in upper Critical Zone silicates and chromitites from 10 m below UG1 to 14 m above UG3 in KF17 core, north of the Steelpoort Lineament (see Fig. 5 for location). Horizontal bars indicate 2σ error for Sr values. Expanded inset illustrates upward decrease in initial ratios from base to top of UG2 chromitite. Source: unpublished data T. Richardson.

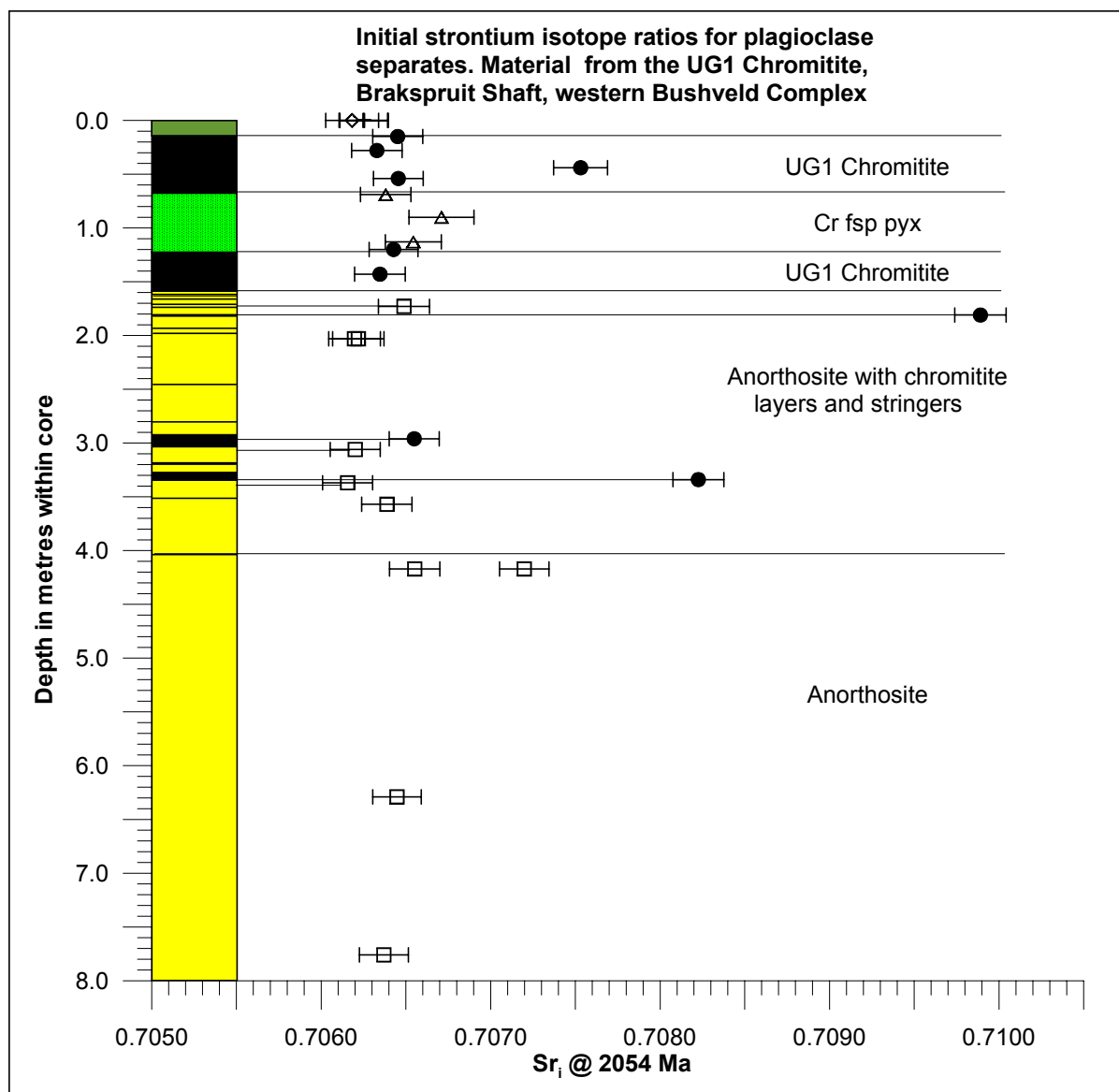


Figure 8: Initial strontium isotope ratio profile through the UG1 chromitite package, footwall anorthosite and hangingwall pyroxenite from BK core, western Bushveld (see Fig. 5 for location). Horizontal bars indicate 2-sigma error for Sr values. Note the high Sr_i ratios in the chromitite-hosted interstitial plagioclase samples, with the highest values in footwall chromitite stringers.

ISOTOPIC RESULTS

More than 80 new Sr analyses have been completed and the data is presented in Figs 6-8 and also in Table 1. For core AM38 (Fig. 6), the plagioclase in the silicate units shows a slight decrease in initial strontium ratio through the succession from c. 0.7063 in the pyroxenite below the LG5 through c. 0.7061 in the anorthosite at the lower/upper Critical Zone boundary to c. 0.7062 above the MG4 (Fig. 6). From 30m depth to the surface (above the

section shown in Fig. 6), the norite has an initial ratio of 0.7060. In contrast, plagioclase, which is interstitial to chromitite, has abrupt, and sometimes extremely high isotopic changes (Fig. 6). Within the LG chromitites the initial strontium ratio varies from 0.7066-0.7070, with the highest ratio of 0.7080 in the MG3 package.

A similar pattern emerges for the UG1 and UG2 chromitites from core KF17 (Fig. 7). The silicate host rocks range in composition from pyroxenite to norite, gabbro-norite and anorthosite. These show typical initial strontium ratios for silicate host rocks through the succession from c. 0.7060 to 0.7064 although a pegmatoidal facies, which occurs in the core at 60 m depth and again at 40 m has elevated strontium ratios (c. 0.7072). However, the highest initial ratios again occur in the chromitites with the highest value of 0.7086 obtained for a plagioclase interstitial to UG1. The high ratios obtained for interstitial plagioclase at the base of the UG2 show a steady decrease through the chromitite to values more typical of host silicates at the top.

Table 1. Data from strontium isotope analysis by thermal ionization mass spectrometry. Sample prefixes in column 1 refer to specific borehole core (AM38, KF-17, BK, and SK9) from this work. Data from samples prefixed 235 are from de Klerk (unpublished) and UG1 data is from Schoenberg et al., (1999). Interstitial plagioclase (Pl (i) and cumulus plagioclase (Pl (c) are distinguished in column 2 and whole-rock samples are also indicated (WR)

Sample No	Analysis	Rb	Sr	$^{87}\text{Rb} / ^{86}\text{Sr}$	$^{87}\text{Sr} / ^{86}\text{Sr}$	$\text{Sr}_i @ 2057 \text{ Ma}$
AM38-42.08	Pl (c)	0.89	492.02	0.00522	0.706354	0.70620 ± 0.00014
AM38-42.72	Pl (i)	4.89	533.81	0.02637	0.706995	0.70621 ± 0.00015
AM38-42.78	Pl (i)	8.06	526.78	0.04404	0.707598	0.70629 ± 0.00016
AM38-42.86	Pl (i)	19.39	510.79	0.10933	0.708926	0.70569 ± 0.00017
AM38-44.74	Pl (i)	1.10	456.94	0.00692	0.706493	0.70629 ± 0.00014
AM38-45.74	Pl (i)	1.74	442.15	0.01132	0.706592	0.70626 ± 0.00015
AM38-46.30	Pl (c)	4.15	320.61	0.03727	0.708688	0.70758 ± 0.00015
AM38-59.49	Pl (c)	2.66	489.37	0.01566	0.706689	0.70623 ± 0.00015
AM38-68.24	Pl (c)	1.94	475.05	0.01176	0.706553	0.70620 ± 0.00015
AM38-71.06	Pl (c)	4.37	483.38	0.02602	0.706808	0.70604 ± 0.00015
AM38-74.51	Pl (c)	3.59	473.41	0.02184	0.706993	0.70635 ± 0.00015
AM38-75.65	Pl (i)	1.76	458.44	0.01107	0.708334	0.70801 ± 0.00015
AM38-76.17	Pl (i)	1.52	416.27	0.01050	0.707113	0.70680 ± 0.00015
AM38-76.36	Pl (c)	4.06	471.89	0.02479	0.706867	0.70613 ± 0.00015
AM38-79.94	Pl (c)	3.48	430.05	0.02328	0.706793	0.70610 ± 0.00015
AM38-80.94	Pl (i)	0.74	393.33	0.00542	0.706491	0.70633 ± 0.00014
AM38-83.67	Pl (i)	1.72	592.66	0.02969	0.706616	0.70574 ± 0.00015
AM38-84.12	Pl (i)	0.77	463.26	0.00481	0.706853	0.70671 ± 0.00014
AM38-84.48	Pl (i)	5.38	877.19	0.01768	0.708175	0.70765 ± 0.00015
AM38-85.18	Pl (i)	1.35	584.04	0.00667	0.706599	0.70640 ± 0.00014
AM38-86.43	Pl (i)	0.29	497.47	0.00143	0.706374	0.70633 ± 0.00014
AM38-91.13	Pl (i)	0.93	449.13	0.00595	0.706378	0.70620 ± 0.00014
AM38-92.20	Pl (i)	2.63	434.11	0.01748	0.706780	0.70626 ± 0.00015

AM38-96.37	Pl (i)	4.90	437.77	0.03226	0.707875	0.70692 ± 0.00015
AM38-96.43	Pl (i)	2.95	459.63	0.01850	0.707067	0.70652 ± 0.00015
AM38-97.07	Pl (i)	2.11	413.22	0.01468	0.707438	0.70700 ± 0.00015
AM38-98.56	Pl (i)	5.15	486.31	0.02975	0.707110	0.70623 ± 0.00015
AM38-99.54	Pl (i)	1.84	441.01	0.01199	0.706923	0.70657 ± 0.00015
AM38-101.46	Pl (i)	14.67	547.42	0.07719	0.708530	0.70624 ± 0.00017
AM38-102.54	Pl (i)	2.81	491.40	0.01646	0.706850	0.70636 ± 0.00015
KF-17-6.65	Pl (i)	0.77	508.05	0.00442	0.706686	0.70656 ± 0.00014
KF-17-6.91	Pl (i)	0.77	597.67	0.00377	0.706432	0.70632 ± 0.00014
KF-17-7.08	Pl (i)	0.75	516.98	0.00424	0.706828	0.70670 ± 0.00014
KF-17-12.61	Pl (i)	2.62	541.57	0.01409	0.706249	0.70583 ± 0.00015
KF-17-14.41	Pl (i)	0.24	529.87	0.00131	0.706301	0.70626 ± 0.00014
KF-17-14.55	Pl (i)	0.63	516.03	0.00353	0.706302	0.70620 ± 0.00014
KF-17-14.63	Pl (i)	2.25	491.48	0.01335	0.706401	0.70601 ± 0.00015
KF-17-15.75	Pl (c)	1.01	502.86	0.00586	0.706611	0.70644 ± 0.00014
KF-17-32.97	Pl (c)	2.46	471.51	0.01518	0.706463	0.70601 ± 0.00015
KF-17-37.96	Pl (i)	0.23	520.11	0.00130	0.706171	0.70613 ± 0.00014
KF-17-38.23	Pl (i)	0.50	536.43	0.00270	0.706402	0.70632 ± 0.00014
KF-17-38.43	Pl (i)	0.79	561.64	0.00409	0.706563	0.70644 ± 0.00014
KF-17-38.59	Pl (i)	0.09	610.48	0.00043	0.706397	0.70638 ± 0.00014
KF-17-38.73	Pl (i)	1.07	483.73	0.00643	0.707096	0.70691 ± 0.00014
KF-17-38.89	Pl (i)	1.54	484.19	0.00925	0.707788	0.70751 ± 0.00014
KF-17-39.00	Pl (i)	0.29	594.98	0.00142	0.707403	0.70736 ± 0.00014
KF-17-39.21	Pl (i)	0.84	572.94	0.00425	0.707335	0.70721 ± 0.00014
KF-17-59.73	Pl (i)	1.54	536.24	0.00835	0.707519	0.70727 ± 0.00014
KF-17-70.93	Pl (c)	0.71	463.13	0.00448	0.706778	0.70665 ± 0.00014
KF-17-88.00	Pl (i)	4.26	344.72	0.03602	0.708355	0.70729 ± 0.00015
KF-17-99.09	Pl (i)	0.68	444.10	0.00449	0.707933	0.70780 ± 0.00014
KF-17-108.62	Pl (i)	52.16	279.81	0.54340	0.711720	0.69561 ± 0.00030
KF-17-109.46	Pl (i)	1.69	440.95	0.01116	0.706557	0.70623 ± 0.00015
KF-17-109.76	Pl (i)	6.52	524.20	0.03625	0.709693	0.70862 ± 0.00015
KF-17-109.86	Pl (c)	2.83	529.42	0.01560	0.708600	0.70814 ± 0.00015
KF-17-110.16	Pl (c)	0.94	471.39	0.00580	0.706483	0.70631 ± 0.00014
KF-17-113.02	Pl (i)	1.00	469.44	0.00620	0.706645	0.70646 ± 0.00014
BKC0.0a	Pl (c)	0.96	476.05	0.00583	0.706426	0.70625 ± 0.00014
BKC 0.0a	Pl (c)	0.99	476.05	0.00599	0.706426	0.70625 ± 0.00014
BKC 0.0b	Pl (i)	6.41	379.06	0.04873	0.707627	0.70618 ± 0.00016
BKC 0.15	Pl (i)	3.14	419.57	0.02155	0.707090	0.70645 ± 0.00015
BKC 0.28	Pl (i)	3.59	426.71	0.02424	0.707047	0.70633 ± 0.00015
BKC 0.44	Pl (i)	8.12	401.95	0.05819	0.709256	0.70753 ± 0.00016
BKC 0.54	Pl (i)	2.45	395.98	0.01778	0.706982	0.70646 ± 0.00015
BKC 0.69	Pl (i)	3.53	372.51	0.02730	0.707190	0.70638 ± 0.00015
BKC 0.90	Pl (i)	20.14	348.99	0.16630	0.711639	0.70671 ± 0.00019
BKC 1.13	Pl (i)	9.60	356.99	0.07744	0.708839	0.70654 ± 0.00017
BKC 1.20	Pl (i)	1.40	435.56	0.00930	0.706703	0.70643 ± 0.00014
BKC 1.43	Pl (i)	3.76	417.99	0.02589	0.707114	0.70635 ± 0.00015
BKC 1.73	Pl (c)	4.85	467.28	0.02988	0.707374	0.70649 ± 0.00015
BKC 1.81	Pl (i)	4.66	430.30	0.03121	0.710816	0.70989 ± 0.00015
BKC 2.03	Pl (c)	5.94	467.21	0.03662	0.707282	0.70620 ± 0.00015
BKC 2.03	Pl (c)	5.82	467.21	0.03586	0.707282	0.70622 ± 0.00015
BKC 2.96	Pl (i)	3.14	440.91	0.02052	0.707157	0.70655 ± 0.00015
BKC 3.06	Pl (c)	3.34	464.74	0.02072	0.706815	0.70620 ± 0.00015
BKC 3.34	Pl (i)	5.28	536.89	0.02834	0.709066	0.70822 ± 0.00015
BKC 3.37	Pl (c)	3.30	462.44	0.02053	0.706764	0.70616 ± 0.00015
BKC 3.57	Pl (c)	3.77	444.10	0.02445	0.707112	0.70639 ± 0.00015
BKC 6.29	Pl (c)	1.24	468.53	0.00765	0.706674	0.70645 ± 0.00015
BKC 7.76	Pl (c)	1.73	471.79	0.01053	0.706682	0.70637 ± 0.00015
235/23	WR	1.09	176.00	0.01794	0.706854	0.70632 ± 0.00015
235/25	WR	6.03	534.00	0.03218	0.707104	0.70615 ± 0.00015
235/29a	WR	8.94	69.20	0.37390	0.718018	0.70694 ± 0.00025

235/29b	WR	9.19	71.00	0.37538	0.717826	0.70670 ± 0.00025
235/30	WR	3.69	62.90	0.16981	0.711917	0.70688 ± 0.00019
235/31	WR	0.74	72.83	0.02941	0.707192	0.70632 ± 0.00015
235/34	WR	5.92	61.90	0.27699	0.714529	0.70632 ± 0.00023
235/35	WR	6.31	52.20	0.35030	0.716654	0.70627 ± 0.00025
SK9-1378.83	WR	0.23	28.84	0.02280	0.707562	0.70689 ± 0.00013
SK9-1379.83	WR	0.27	64.87	0.01180	0.707426	0.70708 ± 0.00013
SK9-1380.30	WR	1.50	23.56	0.18490	0.712395	0.70698 ± 0.00018
SK9-1380.70	WR	0.19	20.98	0.02570	0.707764	0.70701 ± 0.00014
235/37	WR	0.50	66.60	0.02190	0.707318	0.70667 ± 0.00015
SK9-1381.00	WR	0.31	28.97	0.03110	0.707953	0.70704 ± 0.00014
UG2 a	Pl (i)	12.4	372.00	0.09664	0.709577	0.70671 ± 0.00017
UG2 b	Pl (i)	13.4	386.00	0.10079	0.709739	0.70675 ± 0.00017
SK9-1381.17	WR	0.74	42.46	0.05010	0.708647	0.70718 ± 0.00014
SK9-1381.26	WR	0.22	25.09	0.02573	0.707829	0.70708 ± 0.00014
SK9-1381.80	WR	0.41	42.81	0.02766	0.707880	0.70707 ± 0.00014
SK9-1382.45	WR	1.20	28.95	0.11990	0.710059	0.70655 ± 0.00016
UG1	Pl (i)	1.00	84.7	0.0341	0.709293	0.70828 ± 0.00015
SK9-1382.85	WR	0.76	99.67	0.02210	0.707075	0.70643 ± 0.00013
SK9-1382.85	WR	2.42	451.20	0.01552	0.706899	0.70644 ± 0.00013
SK9-1383.30	WR	1.13	471.20	0.00690	0.706462	0.70626 ± 0.00013
SK9-1384.54	WR	1.10	482.00	0.00663	0.706513	0.70632 ± 0.00013

A comparative detailed study of the UG1 from Brakspruit in the western Bushveld shows that plagioclase from anorthosite, chromitiferous pyroxenite and pyroxenite typically has an initial ratio of c. 0.7064. In contrast, interstitial plagioclase from every chromitite analysed shows an initial ratio in excess of the footwall and hangingwall silicates. The highest strontium ratio of 0.7099 was obtained from an anorthosite footwall to the UG1 chromitite (Fig. 8). These values reflect the high initial ratios also obtained on whole rock samples for chromitites in the western Bushveld by Schoenberg et al.⁶⁴

The abnormally high isotope ratios occur mainly within chromitites or in silicate lithologies (chromitiferous pyroxenite or chromitiferous anorthosite) with a significant proportion of streaky chromite. There is a rapid return to 'normal' isotopic compositions in the silicates above the chromitites, and in some cases as in the UG2 at Klipfontein, within the upper portions of the chromitites themselves (see Fig. 7 inset). The origin of the pegmatoids with elevated initial strontium ratios is not clear although the chromitite-bearing pegmatoid at the base of the UG2 shows a significant amount of interaction with the overlying pyroxenite and UG2 and the high isotope ratios in the pegmatoid may have been derived from the high initial Sr ratios at the base of the UG2.

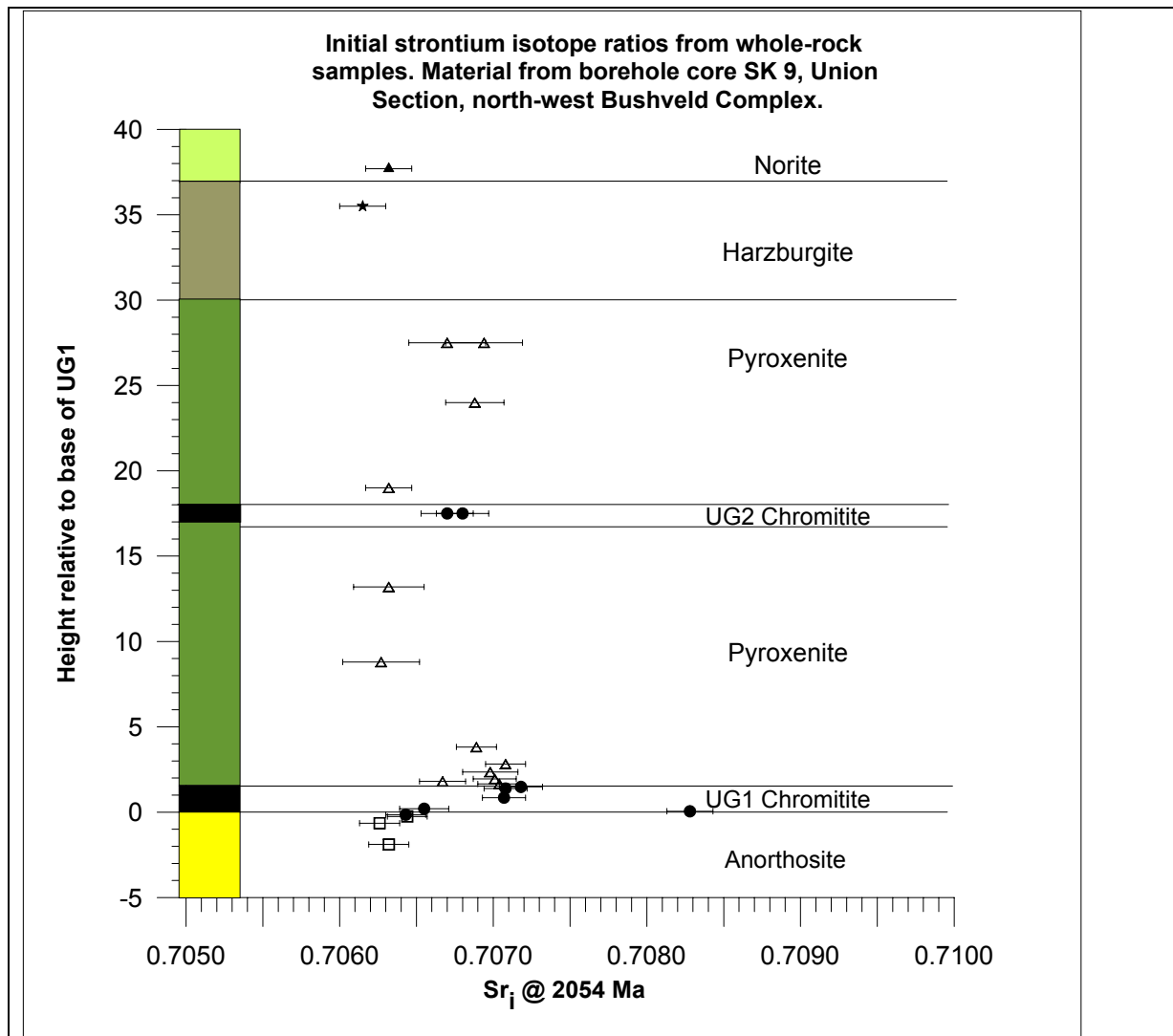


Figure 9: Initial strontium isotope ratio profile for UG1 footwall anorthosite through hanging wall pyroxenite and harzburgite to norite above the UG2. Data from core SK9 Union section northwest Bushveld, de Klerk (unpublished data) and Schoenberg et al, 1999. See Table 1 for details. Horizontal bars indicate 2-sigma error for Sr values.

MODELS FOR THE FORMATION OF CHROMITITES

Previous models

A number of different models have been put forward for the formation of thick chromitite layers, based on evidence not only from the Bushveld Complex but also from Stillwater in particular. Previous models for chromitite formation include:

- (1) gravity-induced separation, crystal sorting and settling⁸¹ has been discounted both on textural evidence,²⁴ on the basis of cotectic proportions²⁵ and on the physics of processes in non-Newtonian magmas;
- (2) immiscibility of Cr-rich liquid⁶² has largely been discounted because of the high temperature (c. 1700°C) at which Cr₂O₃-SiO₂ immiscibility occurs;
- (3) increases in oxygen fugacity by country rock degassing¹² seem unlikely because of the difficulty of controlling such changes over the area of the Bushveld and because

- oxygen fugacity appears to increase systematically from the lowest LG chromitite layer to the uppermost chromitite layers;⁷¹
- (4) contamination by a siliceous component;³⁴
 - (5) mixing between resident and new magma;³⁵
 - (6) lateral growth within a stratified magma column;³⁶
 - (7) pressure changes;¹¹ the fields of spinel and orthopyroxene expand with increasing pressure over a range of 1 to 10kbars at the expense of the olivine and plagioclase fields, so a pressure increase within a magma chamber could result in chromite or orthopyroxene-rich layers, whereas pressure decreases could result in anorthositic or dunite formation. The attraction of this model is that pressure changes could occur simultaneously over the whole magma chamber although the magnitude of change necessary to shift a magma composition from the cotectic into the field of chromite alone is not clear. A pressure change in the order of $\gg 1$ kbar has been suggested.³²; and
 - (8) injection of a chromite-phyric magma²³ still requires that chromite is precipitated somewhere else at greater depth in order to be entrained in the ascending magma.

The various merits of these individual models have been extensively discussed in the literature. However, the sharp contacts and remarkable continuity of some of the chromitite layers require that whatever the process, it must have operated at a sufficient scale to affect the whole chamber at certain periods. Mixing between a primitive and evolved ultrabasic liquid may have resulted in the formation of chromitite layers associated with olivine (LG1-LG4) but for thicker layers associated with orthopyroxene (LG5-MG1) or with orthopyroxene and plagioclase (MG2 and above) mixing between two magmas of very different compositions has been suggested.^{35,36} Different magmas have been proposed for this process e.g. U-type for a magma with a crystallisation sequence of olivine, orthopyroxene, plagioclase, clinopyroxene and A-type for a magma crystallising plagioclase, olivine, clinopyroxene, then orthopyroxene^{30,70}, although recent work shows that there is little evidence for an A-type magma.⁷²

PROPOSED MODEL FOR CHROMITITE FORMATION BASED ON STRONTIUM ISOTOPE DATA

Sr isotope data^{39,27} from the silicate rocks indicate that the Critical Zone had repeated influxes of new magma. However, the transient but extreme isotopic changes associated with the chromitites⁶⁴ shown in this work with rapid return to 'normal' isotopic compositions in the overlying silicates cannot simply have resulted from a new batch of mantle-derived magma contaminated with old crust, because this process would have resulted in large and sustained changes. Any model invoked must account for sudden and stratigraphically localised increases in Sr ratio during chromite formation. Isotopic studies combined with stratigraphic, mineralogical and geochemical data have clarified the dynamics of the magma chamber and the deposition of these major ore bodies and the model proposed here incorporates aspects of more than one of the previously invoked processes namely magma mixing and crustal contamination. The ⁸⁷Sr/⁸⁶Sr data in Figs 6-9, show that the magma from which the chromite formed, usually differed radically from the resident liquid from which the footwall rocks to the chromitites crystallised. The isotopically distinct interstitial plagioclase from many of the chromitite layers indicates that chromite was produced by a sudden and extensive contamination of the magma. The only viable source for this component *in the chamber* is the felsitic roof-rock melt that later consolidated to form granophyre.

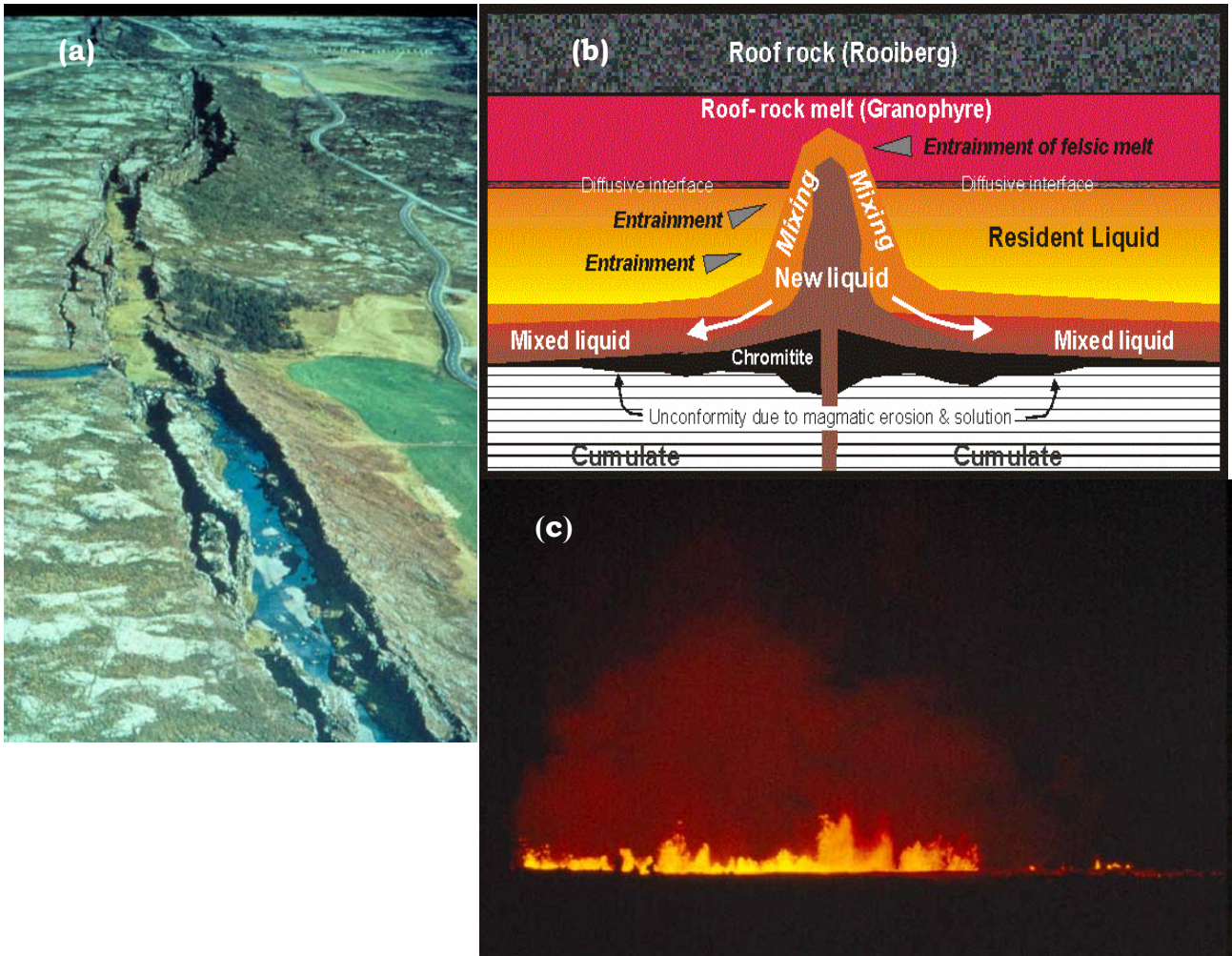


Figure 10: The Mid-Atlantic Ridge on Iceland (a) shows periodic eruptive activity characterised by discontinuous line-fountains of magma (c). A schematic diagram of an envisaged magma intrusion and mixing process is shown in (b). Introduction of a new magma ($Ro = 0.705- 0.706$) as an active fountain resulted in entrainment of resident mafic liquid and if there was sufficient upward momentum, roof rock melt ($Ro > 0.72$) was also entrained. This resulted in contamination by a silica-rich component with the resulting forced crystallisation of chromite and PGM. The mixed liquids were out of equilibrium with the floor cumulates and so reacted and eroded to form an unconformity on to which the chromite-PGM ore was deposited.

It is envisaged that the influxes of new magma (evolved or primitive) erupted into the chamber as fountains along zones of weakness in the crust beneath the chamber. These curtains of magma (or line fountains, are envisaged to have been akin to those that occur along certain zones of the Earth at the present time, eg along the mid-Atlantic Ridge in Iceland (Fig 10a and 10c). When initial momentum was high these line fountains of magma ‘hit the roof’ incorporating a component of melted roof as well as interacting with the resident liquid by entrainment (Fig. 10b). Contamination by such a Si-rich component immediately induced chromite saturation³⁵ within the fountain and chromite then cascaded to

the floor, together with a small amount of magma adherent to the chromite or entrained within the fountain⁷⁵ to produce interstitial silicates with enriched isotopic ratios.

Contamination by the felsic roof melt only continued for as long as the energy in the fountain allowed magma to reach the roof, and as the ‘eruptive’ momentum waned the fountain only penetrated the resident liquid. Thus the dominant process over a prolonged period became one of magma mixing. For the fountains to penetrate the entire thickness of resident magma, the residual CZ melt cannot have been very thick, but at this stage the succeeding magmas (including the Main and Upper Zones) had not yet been intruded. A cloud of chromite crystals collapsed from the head of the fountain to the base of the chamber and it is envisaged that this chromite-rich slurry could have flowed down a 2° slope, in much the same way as a turbidite flows down a continental slope. The flow would have been energised by continued crystallisation of chromitite close to source, with fluidity promoted by the rounded form of the chromite crystals.

These high Sr initial ratios at the base of some chromitites represent a phase of contamination by felsic roof material during the initial fountain surge with later chromitite showing lower Sr initial ratios originating by a magma mixing process. Chromitites, which do not show elevated initial Sr ratios e.g., UG3 (Fig. 7), formed from magma mixing without significant contamination, either because the emplacement of the new batch of magma was less dynamic or because of density contrasts between the new and resident magma.

This proposed model implies repeated magma influxes in the C_LZ and C_UZ with each of the chromitites representing the product of a magma mixing process. The three components are: the intruding magma, the resident magma in the chamber (which is itself a mixture), and the felsic melt floating on the top of the intrusion. It is assumed in the model that it is possible for chromitite layers to spread laterally for significant distances, and transgress across the footwall. Since the base of each major chromitite layer represents a point at which the magma chamber expanded vertically and laterally and there was some deformation and erosion of the footwall rocks, these positions are sub-magmatic unconformities related to both magmatic erosion and loading by the new liquid. The base of the major chromitite layers (and the Merensky Reef) therefore represent para-unconformities within the magmatic stratigraphy.

DISCUSSION

Although Irvine³⁴ proposed contamination by a siliceous (granitic) component, he later argued against this mechanism³⁵ suggesting that considerations concerning alkalis made the granitic magma hypothesis untenable. However, his original argument does apply. Whereas he considered that basic magma would suddenly incorporate a siliceous melt and would create a compositional mixture somewhere between a granite and a basic magma, this model envisages a dynamic evolutionary process whereby the amount of basic magma that is contaminated is actually very small in terms of volume, but the amount of contamination of that small batch can be very high (between 20 and 70%⁶⁴).

Indirect evidence for chromitite formation being due to the influx of new magma is provided by the appearance of potholes in chromitite layers. Recent work on the Merensky Reef suggests that potholes are the downward collapse of crystal mush into pull-apart sites resulting from tensional deformation due to the loading effects of major new magma additions.¹⁵ Similar dish-shaped potholes are recorded in the bases of chromitites where layers have slumped down onto footwall units below.^{47,76,77} These potholes generally have a

diameter of 40-50 m with depths varying between 2-10 m, although exceptionally a diameter of 500m and depth of 55m has been recorded on Winterveld.⁷⁷ Repeated influxes of silicate magma into the chamber during Lower and Critical Zone development have been suggested²⁶ based on cycles of increasing Mg# in pyroxene.

Furthermore, recent studies on bifurcations in the UG1,⁵⁶ indicate that the formation of thick chromitite layers may have been episodic rather than a single event which may account for chemical differences and PGE distributions in some UG2 layers, for example at Lonmin (50 km east of Rustenburg), PGE's are concentrated at the base or in the middle of the UG2 chromitite. Also in parts of the eastern Bushveld, the UG2 can be separated into a lower and upper chromitite on the basis of very distinctive textural and modal differences.⁸⁰

Supportive evidence for crustal contamination during chromitite, and Merensky Reef development, is provided by chemical and isotopic evidence. Osmium isotope data from the majority of chromitite and Merensky and Bastard cyclic units show that there was significant addition of ¹⁸⁷Os to the chromitites from the Middle Group upwards.⁶⁴ Schoenberg et al.⁶⁴ concluded on the basis of such Os isotope data that the PGE deposits of the Bushveld Complex appear to have had a significant crustal input, and that the precipitation was induced by the contamination of the residual magma by a SiO₂-rich crustal melt. It is also possible that locally chromite crystallisation occurred due to magma contamination by country rock xenoliths. Underground on the Rowland Shaft at Marikana a thin rim of chromite associated with uvarovite and monticellite has developed around the margin of a calc-silicate xenolith. An example of unequivocal evidence of contamination of Bushveld magma associated with mineralisation comes from the Platreef in the northern lobe of the Bushveld Complex. Stable isotope data^{10,9} indicates a sedimentary-derived sulphur and carbon contribution to the original basic magma whilst $\delta^{18}\text{O}$ data suggests an assimilation of up to 18% dolomite footwall.³¹ Also contamination by Archaean granitoids has resulted in high and variable initial Sr ratio ranging from 0.7104 to 0.7227.^{4,21}

ROLE OF MAGMA MIXING AND CHROMITITE FORMATION IN THE CONCENTRATION OF PGE'S

The proposed model for chromitite formation can also be used to explain the relationship between PGE's and chromitite. Two major hypotheses have been presented to account for PGE enrichment in layered intrusions although neither concept satisfactorily accounts for mineralisation in all the chromitites, the Merensky Reef and the Platreef:

- (1) **magma mixing with downward scavenging by immiscible sulphides.** The common association of PGE's with Ni and Cu sulphide-bearing assemblages worldwide led to an orthomagmatic model in which an immiscible sulphide phase separating from a silicate magma scavenged base and precious metals.^{13,48,54,55} However, there are considerable difficulties in applying this model to the Bushveld Complex because: (a) chromitites are generally sulphide-poor with low base metal content;^{78,74} and (b) there are certain inconsistencies in applying a model of sulphur-saturation to explain the Merensky mineralisation. The most sulphur-enriched layer in the Bushveld Complex contains only c. 1-2% sulphide in only about 1m of the stratigraphy whilst the rest of the CZ and MZ stratigraphy has <0.1%¹⁸ and within a few metres above the Merensky Reef there is very little sulphide present. Cawthorn¹⁷ argues that once a magma has become sulphur-saturated it remains that way even after mixing of a new magma so that the hanging-wall above the Merensky should be sulphur-saturated.

However, the counter-argument is that oxidation caused the removal of Fe and S from the chromitites, although a de-sulphidation process has been dismissed¹⁷ because low base metal abundances suggest that the sulphides were never there. The dearth of sulphide, low base metal abundance and high PGE's requires another model. Rice and von Gruenewaldt⁵⁹ suggested a process of density stratification within a cooling magma column, sulphide- and chromite-saturation with rapid convection leading to chromite and sulphide deposition within each layer by convective scavenging. However, the high strontium ratio spikes at each chromitite layer presented above, do not support this model, which implies a well-mixed system.

- (2) **transport and concentration of PGE's by upward migrating fluids.** Several models depend on the mobility of PGE's in a saline hydrothermal fluid^{1,6} Boudreau and Meurer⁷ envisaged that the hydrothermal fluid was released from the crystallising Bushveld magma during cooling, whereas Mathez⁴⁹ suggested that the scavenging agent was a differentiated magma rather than a fluid. Alternatively, the fluid may have been externally derived from the metasedimentary rocks in the floor of the chamber. Broadly, it is envisaged that this fluid may have partially resorbed PGE's from the layered sequence and deposited them at horizons where an abrupt change in physical or chemical parameters occurred. Although the passage of the fluid would be difficult to monitor, because it would be buffered by the silicate minerals already crystallising from the magma, the enrichment of Cl in apatite and amphibole associated with certain ore horizons has been cited as evidence of this fluid.⁵ However, the model requires the occurrence of PGE-bearing Ni-Cu sulphides throughout the Lower and Critical Zones from which PGE's were dissolved and precipitated at a higher stratigraphic level so that either remaining sulphides should contain a high grade of Cu and Ni, or if the base metals were also mobilised by the fluid and re-precipitated, evidence for localised enrichment of Cu and Ni should occur. However, anomalously rich Ni- or Cu-rich bodies are absent in Lower and Critical Zone rocks. In addition, hydrothermal scavenging wouldn't appear valid for the Platreef near Potgietersrus where the LZ and most of the CZ are missing and the ore body lies directly on sedimentary rocks of the Transvaal Supergroup or Archaean granite with no footwall sequences of mafic igneous rocks from which PGE could have been scavenged. The Platreef contains the largest total PGM content of all of the mineralised layers, even though its grade is generally lower than either the Merensky or UG2, it is typically 30-60 m thick where mined at Sandsloot north of Potgietersrus. As Cawthorn notes,¹⁷ the hydrothermal model would imply that the greater the vertical distance through which the fluid has passed, the more PGE's may have dissolved from the crystal pile, with concomitant higher grade at the level of deposition. Similarly, in a chromatographic separation model,⁷ the degree of PGE enrichment is a function of the length the chromatographic front travels. However, in the Middle Group chromitites the vertical separations between chromitite layers is small, for instance only a few metres separates the MG1 and MG2 yet the MG2 is relatively enriched in PGE's even compared with other chromitites above and below.⁶⁶ In addition, the grade of mineralisation in the Merensky Reef is similar in both the eastern and western lobes, even though the separation between the UG2 and Merensky Reef may be as little as 30 m in the Union Section to 400 m in the eastern Bushveld. It is also difficult to envisage how fluid infiltration could leave a PGE anomaly that is so laterally persistent, consistently at the same stratigraphic level. Based on the assumption that base-, precious-, and semi-metals have different solubilities and partition differently between silicate melts, immiscible sulphides and supercritical fluids. Leshner and Keays⁴⁵ investigated ores of the Bushveld Complex

and suggested that the Ir contents are more consistent with magmatic segregation and hydrothermal modification than with hydrothermal generation.

Models for PGE mineralisation often fail to account for the close association between chromite and PGE enrichment, and place a lot of emphasis on how sulphides form and scavenge PGE. However, the greater part of the PGM present within chromites appear to be in sub microscopic grains of PGE and base metal alloys rather than sulphides, despite the predominance of sulphide phases at the microscopic scale.^{2,63} Capobianco et al.,¹⁴ suggested a chemical affiliation for the PGM and chromite with PGE's substituting in the spinel lattice and exsolving during cooling, although Tredoux et al.,⁷⁴ rejected the model and Maier and Barnes⁴⁸ noted the lack of correlation between abundance of chromite and PGE content. Microtextural and analytical techniques have shown that PGE's in chromites are not incorporated in the crystal structure but occur as discrete PGM inclusions which range in size from a nanometer- to sub-micrometric scale.^{53,63} Hiemstra³³, suggested that small grains of PGM's that had already formed in the magma, preferentially adhered to chromite surfaces, or were enclosed by chromites so that they were co-precipitated. Merkle⁵⁰ suggested that an arsenide immiscible phase capable of concentrating PGE's developed before a sulphide immiscible phase from evidence of laurite and Os-Ir alloys in chromite layers. Tredoux et al.⁷⁴ proposed that the PGE's formed metal clusters consisting of only a few hundred atoms, which were kept in suspension until precipitation was triggered, with stabilisation by the adherence of ligands such as S, Te and As. Such cluster complexes, which tend to be smaller in size than colloidal particles, are important in catalytic compounds⁵⁸ and many clusters containing Pt have been synthesised.⁷³ Comparison of observed PGE concentrations in mafic silicate magmas with their measured solubilities suggests that many natural magmas are close to PGE saturation and could be perturbed into precipitating alloys by magma replenishment, contamination² or by small reductions in their intrinsic oxidation states.⁵³ Chromite incorporates Fe^{3+} and Fe^{2+} with a $\text{Fe}^{3+}/\text{Fe}^{2+}$ ratio always exceeding that of the melt and furthermore incorporates Cr^{3+} to the complete exclusion of Cr^{2+} despite the presence of Cr in both valencies in the silicate melt.⁶⁰ The net loss of Fe^{3+} and Cr^{3+} will result in a boundary layer that is reduced relative to the main magma and since many magmas are close to PGE saturation even small changes in redox state can cause micronuggets of alloy to form throughout the compositional boundary layer.⁵³ Modelling by Mungall⁵³ suggest reduced solubility of trivalent Os and Ru of 22% and divalent PGE's by about 15% in the boundary layer, resulting in far-field PGE diffusion into the boundary layer for as long as chromite growth continued to impose a reduced $f\text{O}_2$ in its boundary layer. Micronuggets dominated by Os and Ru but including all the PGE will be incorporated in the growing chromite crystals. During hiatuses in chromite growth the alloys will react with the melt to form small numbers of relatively large grains of laurite, which will be incorporated into chromites if they begin to grow again in response to random fluctuations during turbulent magma mixing.⁵³

There is therefore a complex interplay between repeated magma influxes, possibly from different sources, roof contamination, fractionation and potential floor contamination. Our model (Fig. 10) which envisages that an influx of a new magma underwent a transient contamination by Si-rich roof melts, mixed with resident magma and precipitated chromite, would also explain PGE enrichment as PGE cluster complexes, or an early formed arsenide/laurite phase. PGM formation was triggered as the physics and chemistry of the magma changed during contamination and mixing. The chromite and PGM's co-precipitated irrespective of the absolute amount of chromite formed. It is the process of mixing and contamination that caused chromite and/or PGM to precipitate. All chromitites are enriched in PGE relative to source rocks and host rocks, although that enrichment may be less in some

layers, for example UG1 and UG3. Enrichment of chromite relative to associated silicate rocks is of the same order of magnitude of PGM in chromitite relative to associated rocks.⁴² It is an important economic implication in this model that PGE concentrations should also be high in chromitite footwall where high Sr initial ratios are associated with wisps of chromite.

The Merensky Reef chromite is restricted to minor layers or stringers of chromitite and does not occur in the overlying Bastard cyclic unit or succeeding Main Zone. The magma that initiated the Merensky Reef was of a fundamentally different composition relative to all the rocks in the footwall as shown by a marked increase in initial strontium ratio. Nevertheless, the processes of contamination and magma mixing still produced PGE mineralisation and chromite, even though the amount of chromite is small, so it is the processes that are important not the composition of the intruding magma, nor the amount of chromite that formed.

There is abundant petrological and isotopic evidence that fluids have played a role in redistributing PGE's¹³ but we would argue that this occurred after the primary precipitation of PGE's as a result of contamination and magma mixing.

CONCLUSIONS

The abundance of chromitite layers indicates frequent replenishment of the chamber with new magma. Introduction of a new magma ($Ro = 0.705 - 0.706$) as an active fountain resulted in mixing of the resident mafic liquid and if there was sufficient upward momentum, roof-rock melt ($Ro > 0.72$) was also entrained. This resulted in contamination by a silica-rich component with the resulting forced crystallisation of chromite. Chromite crystals once formed, descended onto the floor of the chamber moving away from source as a turbidity flow and it is assumed in the model that it is possible for chromitite layers to spread laterally for significant distances. The mixed liquids were out of equilibrium with the floor cumulates and may have eroded the footwall to form an unconformity onto which the chromite ore was deposited. Contamination of new magma influxes, and mixing with resident magma not only caused chromitite formation but also triggered PGM crystallisation. These PGM's were then incorporated in the chromite slurry. It is therefore implied in this model that PGE concentrations should also be high in chromitite footwall where high Sr initial ratios are associated with wisps of chromite. Thus the major PGM and chromitite ore deposits of the Bushveld Complex are unconformity related, and are associated with the addition and mixing of new magma, coupled to simultaneous contamination by siliceous roof-rock melt. Each of the chromitites therefore represents the product of a magma mixing process.

ACKNOWLEDGEMENTS

We are grateful to Avmin for the provision of Core AM38, particularly to Rob Ingram, Sally Bevington and Dorrit de Nooy. Anglo Platinum provided core KF17 to Trevor Richardson, and we are particularly grateful to Gordon Chunnnett for support in all aspects of this work. Rustenburg Platinum Mines of Anglo Platinum, facilitated by Francois Vos and Alan Page, provided the core from Brakspruit. We are grateful to Richard Montjoie for help with the preparation of Fig.5, to Trevor Richardson for discussion and for the use of data from Core KF17. This work was financed by research funds made available from Impala Platinum, Anglo Platinum, and Lonmin mining companies in South Africa.

REFERENCES

1. Balhaus, C.G. and Stumpfl, E.F. 1986. Sulphide and platinum mineralization in the Merensky Reef: evidence from hydrous silicates and fluid inclusions. *Contr. Mineral. Petrol.*, **94**, 193-204
2. Balhaus, C.G. and Sylvester P. 2000. Noble metal enrichment in the Merensky Reef, Bushveld Complex. *J. Petrol.*, **41**, 4, 545-561
3. Barnard, Jacobs and Mellet, 2000. South African platinum mines and mineralisation, 1:300 000 scale map. Barnard, Jacobs and Mellet, Marshalltown 2107, Johannesburg, South Africa.
4. Barton, J.M., Cawthorn, R.G. and White, J. 1986. The role of contamination in the evolution of the Platreef of the Bushveld Complex, *Econ Geol.*, **81**, 1096-1104
5. Boudreau, A.E. 1995. Some geochemical considerations of platinum-group element exploration in layered intrusions. *Explor. Min. Geol.* **4**, 215-225
6. Boudreau A.E. and McCallum, I.S. 1992. Infiltration metasomatism in layered intrusions. An example from the Stillwater Complex, Montana. *J. Volcan Geothermal Res.*, **52**, 171-183,
7. Boudreau, A.E. and Meurer, W.P. 1999. Chromatographic separation of the platinum-group elements, gold, base metals and sulphur during degassing of a compacted and solidifying igneous crystal pile. *Contrib. Mineral. Petrol.*, **134**, 174-185
8. Buchanan, D.L. 1988. Platinum-group element exploration. *Developments in Economic Geology*, **26**, Elsevier, Amsterdam, 184pp
9. Buchanan, D.L. and Rouse, J.E. 1984. Role of contamination in the precipitation of sulphides in the Platreef of the Bushveld Complex. *Trans.Inst. Min. Metall.*, 141-146.
10. Buchanan, D.L., Nolan, J., Suddaby, P, Rouse, J.E., Viljoen, M.J. and Davenport, J. W.J. 1981. The genesis of sulfide mineralisation in a portion of the Potgietersrus limb of the Bushveld Complex. *Econ. Geol.* **76**, 568-579.
11. Cameron, E.N. 1977. Chromite in the central sector, eastern Bushveld Complex, South Africa. *Am. Mineral.* **62**, 1082-1096
12. Cameron, E.N. and Desborough, G.A. 1969. Occurrence and characteristics of chromite deposits – eastern Bushveld Complex. *Econ. Geol. Mon.* **4**, 23-40
13. Campbell, I.H. Naldrett, A.J. and Barnes, S.J. 1983. A model for the origin of the platinum sulfide horizons in the Bushveld and Stillwater Complexes. *J. Petrol.*, **24**, 133-165
14. Capobianco, C.J., Hervig, R.L. and Drake, M.J. 1994. Experiments on crystallinity and partitioning of Ru, Rh and Pd into magnetite and hematite solid solution crystallized from silicate melts. *Chem. Geol.* **113**, 23-43.
15. Carr, H. W., Kruger, F.J., Groves, D.I. and Cawthorn, R.G. 1999. The petrogenesis of Merensky Reef potholes at the Western Platinum Mine, Bushveld Complex: Sr-isotopic evidence for synmagmatic deformation. *Mineral. Deposita.* **34**, 335-347.
16. Cawthorn, R.G. 1997. Controls on platinum mineralisation in the Bushveld Complex, 8th International platinum symposium, South Africa, 28th June-3rd July 1997, p 67-69
17. Cawthorn, R.G. 1999. Platinum-group element mineralization in the Bushveld Complex – A critical reassessment of geochemical models. *S. Afr. J. Geol.*, **102**, 268-281.
18. Cawthorn, R.G. in press Magma mixing models for Merensky-style mineralisation: the fallacy of binary diagrams. *Econ. Geol.*
19. Cawthorn, R.G. and Walraven, F. 1998. Emplacement and crystallisation time for the Bushveld Complex. *J. Petrol.* **39**, 1669-1687.
20. Cawthorn, R.G. and Webb, S.J. 2001. Connectivity between the western and eastern limbs of the Bushveld Complex. *Tectonophysics*, **330**, 195-209.

21. Cawthorn, R.G., Barton, J.M. and Viljoen, M.J. 1985. Interaction of floor rocks with the Platreef on Overysel, Potgietersrus, northern Transvaal. *Econ. Geol.*, **80**, 988-1006.
22. Cousins, C.A. and Feringa, G. 1964. The chromite deposits of the western belt of the Bushveld Complex. In: The geology of some ore deposits in southern Africa. Ed: S.H. Haughton. *Spec. Pub. Geol. Soc. S. Afr.*, **2**, 183-202.
23. Eales, H.V. 2000. Implications of the chromium budget of the Western Limb of the Bushveld Complex. *S.A.J.G.* 103, 141-150.
24. Eales, H.V. and Reynolds, I.M. 1986. Cryptic variation within chromitites of the upper Critical Zone, northwestern Bushveld Complex. *Econ. Geol.* **81**, 1056-1066
25. Eales, H.V. and Cawthorn, R.G. 1996. The Bushveld Complex. In: Layered Intrusions. Ed: R.G. Cawthorn. *Develop. Petrol.* 15, Elsevier. 531pp
26. Eales, H.V., de Klerk, W.J. and Teigler, B. 1990a. Evidence for magma mixing processes within the Critical and Lower Zones of the northwestern Bushveld Complex, South Africa. *Chem. Geol.*, **88**, 261-278.
27. Eales, H.V., de Klerk, W.J., Butcher, A.R. and Kruger, F.J. 1990b. The cyclic unit beneath the UG1 chromitite (UG1FW unit) at RPM Union Section Platinum Mine – Rosetta Stone of the Bushveld Upper Critical Zone. *Min. Mag.* **54**, 23-43.
28. Hall, A.L. and Humphrey, W.A. 1908. On the occurrence of chromite along the southern and eastern margins of the Bushveld plutonic complex. *Trans. Geol. Soc. S. Afr.*, **11**, 69-77.
29. Hamilton, P.J. 1977. Sr isotope and trace element studies of the Great Dyke and Bushveld mafic phase and their relation to early Proterozoic magma genesis in southern Africa. *J. Petrol.*, **18**, 24-52.
30. Harmer, R.E. and Sharpe, M.R. 1986. Field relations and strontium isotope systematics of the marginal rocks of the eastern Bushveld Complex. *Econ. Geol.* **80**, 813-837
31. Harris, C. and Chaumba, J.B. 2001. Crustal contamination and fluid-rock interaction during the Formation of the Platreef, northern limb of the Bushveld Complex, South Africa. *J. Petrol.*, **42**, 7; 1321-1347.
32. Hatton, C.J. and von Gruenewaldt, G. 1989. The geological setting and petrogenesis of the Bushveld chromitite layers. In: Chromite deposits through time. Ed. C. W. Stowe. International Geological Congress, Washington, 109-142.
33. Hiemstra, S.A. 1979. The role of collectors in the formation of the platinum deposits in the Bushveld Complex. *Can. Mineral.* **17**, 469-482.
34. Irvine, T.N. 1975 Crystallization sequences in the Muskox intrusion and other layered intrusions-II. Origin of chromitite layers and similar deposits of other magmatic ores. *Geochimica et Cosmochimica Acta* **39**, 991-1020.
35. Irvine, T.N. 1977. Origin of chromitite layers in the Muskox intrusion and other stratiform intrusions: a new interpretation. *Geology* **5**, 273-277.
36. Irvine, T.N., Keith, D.W. and Todd, S.G. 1983. The J-M platinum-palladium Reef of the Stillwater Complex, Montana: II Origin by double diffusive convective magma mixing and implications for the Bushveld Complex. *Econ. Geol.* **78**, 1287-1334.
37. Kruger, F.J. 1990. The stratigraphy of the Bushveld Complex: a reappraisal and relocation of the Main Zone boundaries. *S. Afr. J. Geol.*, **93**, 376-381
38. Kruger, F.J. 1992. The origin of the Merensky cyclic unit: Sr-isotopic and mineralogical evidence for an alternative orthomagmatic model. *Aust. J. Earth Sci.*, **39**, 255-261.
39. Kruger, F.J. 1994. The Sr-isotopic stratigraphy of the western Bushveld Complex. *S. Afr. J. Geol.* **97** (4), 393-398.
40. Kruger, F.J. and Marsh, J.S. 1982. The significance of $^{87}\text{Sr}/^{86}\text{Sr}$ ratios in the Merensky cyclic unit of the Bushveld Complex. *Nature*, **298**, 53-55.

41. Kruger, F.J. and Schoenberg, R. 1997. Isotope evidence for the origin of PGE rich Bushveld chromitites and the Merensky Reef by Felsic magma mixing. Abstr. 8th Internat. Platinum Symp. 28th June- 3rd July, GSSA, South Afr. 185-188.
42. Kruger, F.J., Kinnaird, J.A. Nex, P.A.M. and Cawthorn, R.G. 2002. Chromite is the key to PGE. Abstr. 9th Internat. Platinum Symp. July, Stillwater, USA.
43. Lee, C.A. 1996. A review of mineralisation in the Bushveld Complex and some other layered intrusions, In: Layered intrusions" Ed. R.G. Cawthorn, Elsevier, pp103-145
44. Lee, C.A. and Parry, S.J. 1988. Platinum group element geochemistry of the lower and middle group chromitites of the eastern Bushveld Complex. *Econ. Geol.*, **85**, 877-883
45. Leshner, C.M. and Keays, R.R. 2002. Discrimination between magmatic and hydrothermal Ni-Cu-PGE and PGE mineralisation. Abstr. 9th Internat. Platinum Symp. July, Stillwater, USA.
46. Li, C., Maier, W.D. and de Waal, S.A. 2001. The role of magma mixing in the genesis of PGE mineralisation in the Bushveld Complex: Thermodynamic calculations and new interpretations. *Econ. Geol.* **96**, 653-662.
47. Lonmin, 2001. A guide to the geology at Lonmin Platinum. Field guide, 10pp.
48. Maier, W.D. and Barnes, S-J. 1999. Platinum-group elements in silicate rocks of the Lower, Critical and Main Zones at Union section, western Bushveld Complex. *J.Petrol.* **40**, 1647-1671.
49. Mathez, E.A. 1995. Magmatic metasomatism and formation of the Merensky reef, Bushveld Complex. *Contrib. Mineral. Petrol.*, **119**, 277-286.
50. Merkle, R.K.W. 1992. Platinum-group minerals in the middle group of chromitite layers at Marikana, western Bushveld Complex: indications for collection mechanisms and post-magmatic modification. *Can. J. Earth Sci.* **29**, 209-221.
51. Mitchell, A.A. 1990. The stratigraphy and mineralogy of the Main Zone of the northwestern Bushveld. *S. Afr. J. Geol.*, **93**, 818-831.
52. Molyneux, T.G. 1974. A geological investigation of the Bushveld Complex in Sekhukhuneland and part of the Steelpoort Valley. *Trans. Geol. Soc. S. Afr.*, **77**, 329-338.
53. Mungall, J, 2002. A model for co-precipitation of platinum-group minerals with chromite from silicate melts. Abstr. 9th Internat. Platinum Symp. July, Stillwater, USA.
54. Naldrett, A.J. 1989a. Stratiform PGE deposits in layered intrusions. *Rev. Econ. Geol.*, **4**, 135-166
55. Naldrett, A.J. 1989b. Magmatic sulfide deposits. Oxford Monographs on Geol. and Geophys. 14, Oxford University Press, 186pp
56. Nex, P.A. 2002. The UG1, characteristics and causes. Spinel (chromium, vanadium, titanium and iron) geology, chemistry, extraction and uses. Short course abstracts, Bushveld Branch of the Geol. Soc. S. Afr. 5-6th February, Mooi-nooi, South Africa.
57. Nex, P.A., Kinnaird, J.A., Ingle, L.J., van der Vyver, B.A. and Cawthorn, R.G. 1998. A new stratigraphy for the Main Zone of the Bushveld Complex, in the Rustenburg area. *S. Afr. J. Geol.*, **101**(3), 215-223
58. Okafor, V.I. and Coville, N.J. 1999. Platinum in catalysis. *S. Afr. J. Sci.*, **95**, 503-508.
59. Rice, A. and von Gruenewaldt, G. 1975. Convective scavenging and cascade enrichment in Bushveld Complex melts: possible mechanisms for concentration of platinum-group elements and chromite in mineralised layers. *Trans. Inst. Min. Metall.* **103**, B31-38
60. Roeder, P.L. and Reynolds, I. 1991. Crystallization of chromite and chromium solubility in basaltic melts. *J. Petrol.*, **32**, 909-934

61. SACS, 1980. South African Committee for Stratigraphy (SACS). Stratigraphy of South Africa. Part 1 (Comp. L.E. Kent). Lithostratigraphy of the Republic of South Africa. *Handbk. Geol. Surv. S. Afr.*, **8**, 690 pp
62. Sampson, E. 1932. Magmatic chromitite deposits in Southern Africa. *Econ. Geol.* **27**, 113-144
63. Sattari, P., Brenan, J.M. McDonough, W.F. and Horn, L. 1999. Chromite melt partitioning of Re and the PGE's. GAC-MAC Program with abstracts **24**, 109, Sudbury.
64. Schoenberg, R., Kruger, F.J., Nagler, T.F., Meisel, T. and Kramers, J.D. 1999. PGE enrichment in chromitite layers and the Merensky Reef of the western Bushveld Complex; a Re-Os and Rb-Sr isotope study. *Earth and Planetary Science Letters* **172**, 49-64.
65. Schürmann, L.W., Grabe, P-J and Steenkamp, C.J. 1998. Chromium. In Wilson, M.G.C. and Anhaeusser, C.R. (eds.), *The mineral resources of South Africa: Handbook*, Council for Geoscience, 16, 740pp
66. Scoon, R.G. and Teigler, B. 1994. Platinum Group element mineralisation in the Critical Zone of the western Bushveld Complex: 1. Sulphide-poor chromitites below the UG2. *Econ. Geol.*, **89**, 1094-1121
67. Scoon, R.G. and Teigler, B. 1995. A new LG6 chromite reserve at Eerste Geluk in the boundary zone between the central and southern sectors of the eastern Bushveld Complex. *Econ. Geol.*, **90**, 969-982
68. Sharpe, M.R. 1982. The floor contact of the eastern Bushveld Complex: field relations and petrography. Inst. for geol. res. on the Bushveld Complex, *Research. Rep. 36*, Pretoria, Univ. Pretoria. 43pp.
69. Sharpe, M.R. 1985. Strontium isotope evidence for preserved density stratification in the Main Zone of the Bushveld Complex, South Africa. *Nature*, **316**, 119-126.
70. Sharpe, M.R. and Irvine, T.N. 1983. Melting relations of two Bushveld chilled margin rocks and implications for the origin of chromitite. *Yearbook Carnegie Inst.* Washington, **82**, 295-300
71. Teigler, B. and Eales, H. V. 1993. Correlation between chromite composition and PGE mineralisation in the Critical Zone of the western Bushveld Complex. *Min. Dep.* **28**, 291-302
72. Teigler, B. and Eales, H. V. 1996. The Lower and Critical Zones of the western limb of the Bushveld Complex as intersected by the Nooitgedacht borehole. *Bull. Geol. Surv. S. Afr.* **111**, 126 pp.
73. Toshima, N., Nakata, K. and Kitoh, H. 1997. Giant platinum clusters, with organic ligands, preparation and catalysis. *Inorg. Chim. Acta* **265**, 149-153.
74. Tredoux, M., Lindsay, N.M. Davies, G. and MacDonald, I. 1995. The fractionation of platinum-group elements in magmatic systems with the suggestion of a novel causal mechanism. *S. Afr. J. Geol.* **98**, 157-167
75. Turner, J.S. and Campbell, I.H. 1986. Convection and mixing in magma chambers. *Earth Sci. Rev.* **23**, 255-352
76. Viljoen, M.J. and Hieber, R. 1986. The Rustenburg section of Rustenburg Platinum Mines Limited, with reference to the Merensky reef. In: C. R. Anhaeusser and S. Maske, Eds. *Mineral Deposits of southern Africa*. Geol. Soc. S. Afr. Johannesburg, 1107-1134.
77. Viljoen, M.J. and Schürmann, L.W. 1998. Platinum-group metals. In: M.G.C. Wilson and C.R. Anhaeusser, eds. *The mineral resources of South Africa*. Council for Geosciences Handbk. **16**. 740 pp

78. von Gruenewaldt, G and Merkle, R.K.W. 1975. Platinum group element proportions in chromitites of the Bushveld Complex: implications for fractionation and magma mixing models. *J. Afr. Earth Sci.*, **21**, 4, 615-632
79. von Gruenewaldt, G., Hatton, C.J., Merkle, R.K.W. and Gain, S.B. 1986. Platinum group element-chromitite associations in the Bushveld Complex. *Econ. Geol.* **81**, 1067-1079.
80. von Gruenewaldt, G., Dicks, D., de Wet, J and Horsch, H. 1990. PGE mineralisation in the western sector of the eastern Bushveld Complex. *Research. Rep. Instit. For Geol. Res. on the Bushveld Complex*, **80**, Univ. Pretoria. 37pp
81. Wager, L.R. and Brown, G.M. 1968. *Layered igneous rocks*. Oliver and Boyd, Edinburgh. 588pp
82. Wagner, P.A. 1929. *The platinum deposits and mines of South Africa*. Oliver and Boyd, Edinburgh, 326pp
83. White, J.A. 1994. The Potgietersrus project: geology and exploration history. Proc 15th CMMI Congress. S. Afr. Inst. Min. Metall., Johannesburg, S. Afr. 173-182.
84. Wilson, J.R., Cawthorn, R.G., Kruger, F.J. and Grundvig, S. 1994. Intrusive origin for the unconformity in the northern Gap, western Bushveld Complex. *S. Afr. J. Geol.*, **97**, 462-472.

_____oOo_____

About the author's

J. A. Kinnaird obtained her MSc and PhD from the University of St. Andrews, Scotland for studies on the alteration and mineralisation of alkaline ring complexes in Nigeria. She has been a geological consultant practising with GeoMetallica Ltd. She is currently a senior research fellow within the Economic Geology Research Institute at the University of Witwatersrand working on mineralisation and magmatic processes in the Bushveld Complex, gemstones in Pan-African terranes and mineralisation in the Lufilian and Damaran orogenic belts.

F. J. Kruger is a graduate of The University of Natal (BSc (Hons) 1975) and Rhodes University (MSc 1978, PhD 1983). He taught at the University of Cape Town (1982/3) and joined the University of the Witwatersrand in 1984 and is with the Economic Geology Research Institute - Hugh Allsopp Laboratory. He is a specialist in applications of isotope chemistry to geology and petrology, economic geology, archaeological and environmental tracing and tagging (tuskprinting).

P. A. M. Nex graduated from Oxford Brookes University in 1991. He completed a Ph.D. at University College Cork, Ireland on the tectono-metamorphic setting of uraniferous sheeted granites in the Damara Orogen, Namibia. Since then he has worked as a consultant on projects in Namibia, South Africa, and Ireland and is currently a research fellow at the University of the Witwatersrand working on magmatic processes in the Bushveld Complex.

R.G. Cawthorn obtained a BSc from Durham University and PhD from Edinburgh University and for 27 years has worked at the University of the Witwatersrand in South Africa. Most of his research has been on the Bushveld Complex, and he teaches igneous petrology. For the last five years his position has been subvented by Anglo Platinum, Impala Platinum and Lonmin (Platinum), and has the title of the Platinum Industry's Professor of Igneous Petrology.